Alluvial gravel sedimentation in a contractional growth fold setting, Sant Llorenc de Morunys, southeastern Pyrenees

Alluvial gravel sedimentation in a contractional growth fold setting, Sant Llorenc de Morunys, southeastern Pyrenees

Article *in* Geological Society London Special Publications · January 1998

DOI: 10.1144/GSL.SP.1998.134.01.05

CITATIONS
26

READS
107

4 authors, including:

Mary Ford
University of Lorraine
108 PUBLICATIONS **2,712** CITATIONS
SEE PROFILE

Jaume Vergés
Geosciences Barcelona (Geo3Bcn) CSIC
310 PUBLICATIONS **9,783** CITATIONS
SEE PROFILE

Andrea Artoni
Università di Parma
67 PUBLICATIONS **1,012** CITATIONS
SEE PROFILE

Cenozoic Foreland Basins of Western Europe

Geological Society
Special Publication
No. 134

edited by A. Mascle, C. Puigdefàbregas, H. P. Luterbacher and M. Fernàndez

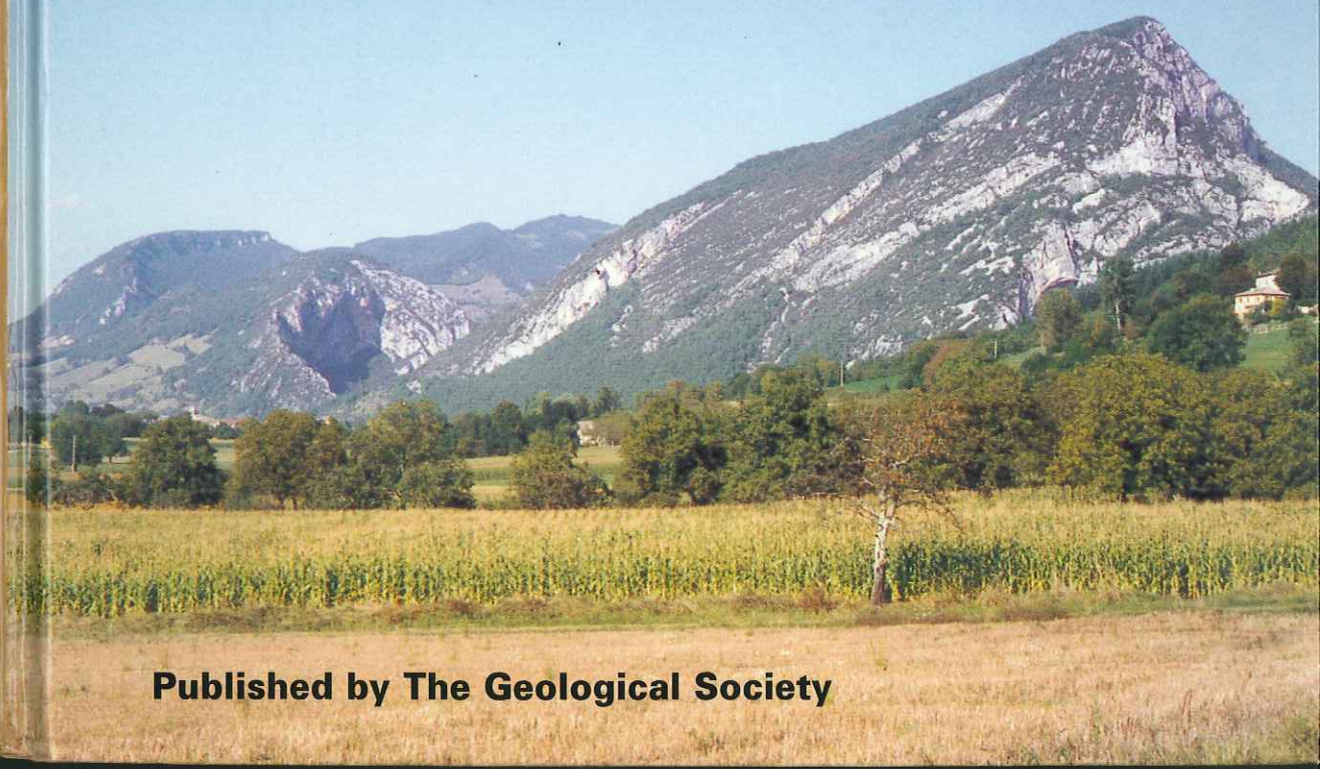

Published by The Geological Society

Alluvial gravel sedimentation in a contractional growth fold setting, Sant Llorenç de Morunys, southeastern Pyrenees

EDWARD A. WILLIAMS[1], MARY FORD[1], JAUME VERGÉS[2] & ANDREA ARTONI[1]

[1]*Geologisches Institut, ETH-Zentrum, CH-8092 Zürich, Switzerland (e-mail eaw@erdw.ethz.ch)*

[2]*Institute of Earth Sciences "Jaume Almera", Consejo Superior de Investigaciones Científicas, Lluís Solé i Sabarís s/n, 08028 Barcelona, Spain*

Abstract: New data are presented on the classic growth structure at Sant Llorenç de Morunys (NE Ebro Basin, Spain). During the late Eocene to Oligocene thick alluvial-fan gravel sediments accumulated principally by repetitive sub-aerial mass flow (cohesionless debris flow and fluidal sediment flow) events, with smaller volumes of fan-stream flows. Subaerial, high-viscosity (cohesive) debris flows contributed comparatively small volumes of sediment to the successsion. These sediments constructed a complex architecture of conglomeratic and sandstone-bearing lithosomes that were affected by stratal thickening and erosion across a growth fold pair and genetically related internal unconformities, which formed a long-lived thrust-related structure in the immediate footwall of the SE Pyrenean mountain front. Four periods of evolution for the Sant Llorenç growth structure are defined on the basis of distinctive stratigraphical architecture. These describe a gross evolution from onlapping to overlapping growth strata, related to the ultimate demise of growth folding. In detail complex erosional and offlapping events punctuated the growth history, which shows extreme variation parallel to the axis of the structure. Patterns of palaeoflow were highly complex, showing distinct axial and transverse directions relatable to growth fold evolutionary periods. Palaeocurrents are considered to have been deflected and diverted by surficial differential subsidence and areas of relative uplift and erosion generated by fold growth. The complexity of sediment dispersal is compounded by variables intrinsic to alluvial fan environments. The Sant Llorenç de Morunys growth strata provide information on how sediments are reorganized by syndepositionally-growing structures and on the nature of sediment distribution between external fold-and-thrust belts and foreland basins.

Gravelly sediments shed from the erosion of collisional orogens are trapped in the proximal zones of flexural foreland basins in several distinct depositional environments. Commonly, where continental (alluvial) settings are developed over a wide zone up to the mountain front, proximal conglomerates may accumulate in bajadas comprising steep, small-radius alluvial fans, but also, synchronously, in the channel belts of gravelly braided rivers which transfer large volumes of coarse and fine sediment across foreland basins. Where continental settings are restricted due to marine or lacustrine flooding of the foreland basin, gravels accumulate in fan-deltas (Nemec & Steel 1988) or as river-dominated braid-deltas (McPherson *et al.* 1987) supplying clastic material to coarse-grained coastal environments (Nemec & Steel 1984). Where continental environments predominate, the gravel reaches of permanent river channels, at spaced exits from the mountain belt (Hovius 1996), coincide with the coarse-grained proximal-medial zones of steep fans, posing problems of distinction between environments (e.g. Hirst & Nichols 1986; Nichols 1987*a*; see also Haughton 1989; Nemec & Postma 1993; Blair & McPherson 1994*a*). As well as providing signatures of thrusting, uplift, erosion and drainage reorganization in the source area (Blair & Bilodeau 1988; Burbank *et al.* 1988; Colombo 1994; Gupta 1997) and subsidence regimes within the basin (Paola 1988, 1989; Paola *et al.* 1992; Whipple & Trayler 1996), gravel sediments in proximal foreland basin settings are themselves deformed by thrusting and folding during their accumulation. Active deformation of the aggradational area may episodically or quasi-continuously affect the topography with resultant effects on water–sediment dispersal, erosion (with the creation of new drainage routeways) and gross stratigraphical development. Tectonic deformation of the sediments accumulating at mountain fronts gives rise to so-called growth structures, with their associated

WILLIAMS, E. A., FORD, M., VERGÉS, J. & ARTONI, A. 1998. Alluvial gravel sedimentation in a contractional growth fold setting, Sant Llorenç de Morunys, southeastern Pyrenees. *In*: MASCLE, A., PUIGDEFÀBREGAS, C., LUTERBACHER, H. P. & FERNÀNDEZ, M. (eds) *Cenozoic Foreland Basins of Western Europe*. Geological Society Special Publications, **134**, 69–106

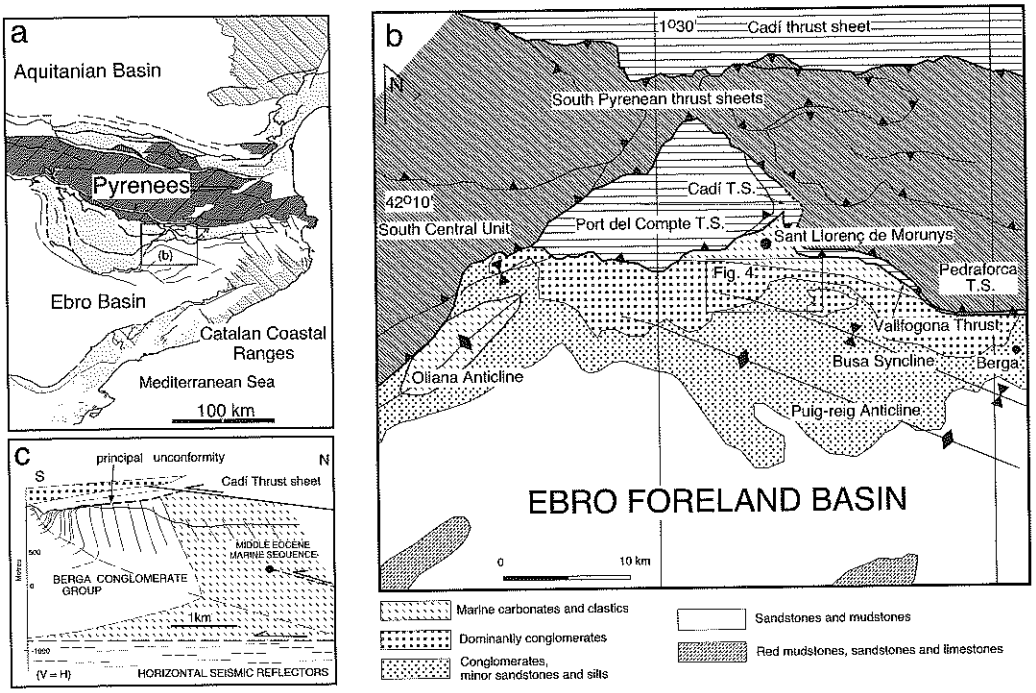

Fig. 1. (**a**) Tectonic map of the eastern Pyrenees and Ebro Basin, showing the location of (b). The Pyrenean axial zone is shown by the dark-shaded hatching. (**b**) Map showing the distribution of Late Eocene–Oligocene continental clastic facies (based on the 1:250 000 geological map of Catalunya), and major structures of the foreland basin in the Sant Llorenç de Morunys area. Studied area is boxed. (**c**) Local N–S cross section showing the deep structural context of the Sant Llorenç de Morunys growth fold (central part), and its relationship to the frontal emergent thrust of the SE Pyrenees which is sealed by the upper units of the Berga Conglomerate Group (coarse stipple).

suite of progressive unconformities (Riba 1976*b*; Anadón *et al.* 1986) and growth strata geometries (Artoni & Casero 1997; Ford *et al.* 1997; Suppe *et al.* 1997). Evolving topography will distort classical radial dispersal patterns of steep alluvial fans, and potentially deflect or divert more permanent river courses, unless conditions favouring antecedent drainage across structures are met (Burbank *et al.* 1996). Drainage basins associated with actively deforming zones at mountain fronts are commonly multiple in origin (Friend 1989), and the material they yield will partially accumulate within growth structures developed in this zone.

Growth structures, their associated stratal geometries, sedimentology and petrographic evolution have been widely studied (e.g. Rockwell *et al.* 1985; DeCelles *et al.* 1991*a*, *b*, 1995; Mellere 1993) and particularly around the margins of the Eo-Miocene Ebro Basin, Spain (Riba 1967, 1976*a*, *b*; Anadón *et al.* 1986; Nichols 1987b; Vergés & Riba 1991; Colombo & Vergés 1992; Burbank *et al.* 1992*a*, *b*, 1996; Millán *et al.* 1994; Burbank & Vergés 1994; Vergés *et al.* 1996). Some recent key studies of the interaction between alluvial systems and developing structures in foreland basin settings have concentrated on theoretical explanations of drainage diversion by folds (Burbank *et al.* 1996), control due to break-back sequences of thrusts associated with detachment folds (Burbank & Vergés 1994) and drainage basin reorganization and megafan location due to frontal thrust propagation and fold growth (Gupta 1997). In this paper, we focus on the growth structure near Sant Llorenç de Morunys (see Riba 1973, 1976*a*, *b*), which preserves complex fold and stratal geometries developed in the immediate footwall of the late Eocene–Oligocene SE Pyrenean mountain front (Fig. 1a). This fold pair developed over a long period below the surface of the foreland basin, providing localized accommodation space, but otherwise having a more subtle influence on sedimentary processes than previously described growth folds. The study aims to

document and explain the interaction of the coeval fold growth, gravel sedimentation and dispersal, surface erosion and stratigraphical development by integrating interpreted sedimentary processes and environments with a series of palaeogeographical–tectonic maps of the evolving basin margin. The latter have been constructed from sequential restorations of serial cross sections through the growth structure (Ford *et al.* 1997). Sediment dispersal has been investigated by the measurement of a suite of palaeocurrent indicators across the structure.

Geological setting

The Sant Llorenç de Morunys growth structure affects Eocene–Oligocene conglomerates (and minor interbedded sandstones) up to 5 km south of the east–west-trending Vallfogona Thrust (Fig. 1b), and persists laterally for approximately 25 km. A variable width fringe of conglomerates characterizes this part of the NE Ebro Basin, from the northern flank of the Oliana growth fold at the SE margin of the south-central unit (Burbank & Vergés 1994) to the coarse-grained alluvial dispersal systems in the Berga area (Mató *et al.* 1994; Fig. 1b). The very low-angle (7°) frontal emergent (Vallfogona) thrust emplaces the Port del Compte and Cadí thrust sheets (consisting mainly of thin Mesozoic and thick lower to middle Eocene shallow-water limestones and marls) towards the SSW (Vergés 1993), over mid Eocene shallow marine clastic-carbonate shoreline and coastal plain sediments (equivalent to the Banyoles and Igualada Marl Formations, Vergés 1993), and the alluvial Berga Conglomerate Group. These rocks define a large-scale growth fold pair which developed as a fault propagation fold ahead of a footwall splay of the Vallfogona thrust (Fig. 1c; Ford *et al.* 1997, fig. 3a). On a seismic profile horizontal reflectors indicate that the fold pair is detached on a thrust flat at depth (Fig. 1c). This thrust accommodates *c.* 8 km of southward displacement, and the minimum displacement accommodated by the Vallfogona thrust is estimated to be 8.4 km (Vergés 1993). The true displacement is difficult to define as no clear stratigraphical correlation can be made across the thrust. The Vallfogona thrust is, however, buried by conglomerates of the upper Berga Group to the west of Sant Llorenç, and would appear to be the principal mountain-front structure which influenced sedimentation in the Sant Llorenç de Morunys area. Traced to the south, the proximal Berga Group conglomerates become finer-grained and more thinly bedded, replaced by finer grained facies (sandstones and siltstones) in the succession (Fig. 1c). Conglomerates extend *c.* 5 km beyond the trace of the Puig-reig growth ramp anticline (Vergés 1993), where they are replaced by sandstones and mudstones (Fig. 1b).

On a larger scale the Port del Compte and Cadí thrust sheets are part of a stack of thrust sheets that are preserved above foreland basin deposits. These are bounded to the north by the axial zone of the Pyrenees (Fig. 1a) which comprises Upper Palaeozoic low-grade metasediments and Variscan plutons. Regional balanced sections constructed across the SE Pyrenean thrust belt reveal a shortening of *c.* 150 km in the central part (Muñoz 1992) and 125 km in the eastern part (Vergés 1993). The major period of emplacement of the thrust sheets in this region of the orogen (latest Cretaceous to Oligocene), and the Eocene–Oligocene age of the sediments that seal the Vallfogona thrust indicates that the sediment transport path for the Berga Group from known source areas in the axial zone (Riba 1976*b*) was approximately the present-day distance (Fig. 1a). The Berga Conglomerate Group represents the waning stages of foreland basin sedimentation in the NE Ebro Basin, although Miocene alluvium accumulated in western-central areas. The late Eocene closure of the Ebro Basin to become an area of centripetal drainage (Riba *et al.* 1983) led Coney *et al.* (1996) to suggest that the Berga Group was continuous with conglomerates which 'backfilled' the southern Pyrenean fold and thrust belt, the evidence for which has been challenged by González *et al.* (1997).

Local stratigraphical-structural setting of the conglomerates

An internal lithostratigraphy of the Berga Conglomerate Group at Sant Llorenç de Morunys is presented in Fig. 2, which is based on field mapping and sequence logging of distinguishable units of different scale (see Ford *et al.* 1997). The base of the Berga Group is an abrupt conformable transition, occurring over some 10–15 m, from interbedded marine marls, sandstones, rare nummulitic limestones and essentially non-reddened pebble–cobble conglomerates, to stacked, thick conglomerates associated with finer-grained reddened sediments. The mid-Eocene biostratigraphy of the upper marine sediments, suggests a late Eocene age for the lower Berga Conglomerates (Riba 1973), although no more accurate dating is currently available.

Previous stratigraphical work (Riba 1976*a*, *b*) divided the Berga conglomerates into four members based on several 'conglomeratic key beds' that were traced from aerial photographs. These key beds, on examination, comprise metre-scale bedsets of conglomerates and sandstones, and are thus multiple event deposits, often found to form part of new mapping divisions. The new scheme (Fig. 2) defines a series of geometrically complex conglomeratic and sandstone-rich formational units. A simplified measured section through some of these units (Fig. 2) is shown in Fig. 3, emphasizing the differentiation of the succession and constituent lithosomes by bulk grain size. Overall, all formations are dominated by conglomerate lithologies (Fig. 3), whereas those units designated sandstone-rich (Fig. 2) contain *c.* 20–30% of sandstone or pebbly sandstone lithologies. Several instances of bulk facies changes occur in depositional-strike parallel directions (WNW–ESE to E–W), which result in the pinching out or sharper termination of conglomerate-dominant formations (Figs 2 & 4). Some units have subtle triangular cross-sections on a scale of >2 km, suggesting that they have wedge- or lobate-forms in three-dimensions, similar to geometries of gravelly alluvial fan deposits described by Koltermann & Gorelick (1992, fig. 3). These geometrical attributes indicate that the formations comprise large-scale lithosomes in the sense of Wheeler & Mallory (1956). Geometrical complexity also occurs within units designated as formations. In the dip-parallel direction, more marked thickness changes occur, which are clearly relatable to the axial surfaces of the growth folds (see below and Fig. 5).

The growth structure (Fig. 4) can be divided into (1) a northern 3 km thick, overturned to sub-vertical panel comprising the marine clastic–carbonate succession and lower alluvial conglomerates (Casa Blanca, El Castell and Sobirana Formations, Fig. 2) and (2), in the south, a growth fold pair, comprising the upper alluvial conglomerates (Camps de Vall-llonga, Pont de les Cases to Mirador Formations). The steep panel and fold structures to the south are considered (Ford *et al.* 1997) to be part of a single large growth fold pair as shown in Fig. 1c that grew continuously during deposition of the Berga Conglomerate Group (see Suppe *et al.* 1997 for an alternative interpretation). The steep panel can be traced for over 25 km eastward from Coll de Jou (Fig. 4). Three cross sections through the area (Ford *et al.* 1997; Fig. 5) show that the geometry of the growth fold varies along strike. On the western flank of Vall de Lord (profile 1; Figs 5a & 6a) these two structural zones are separated by a spectacular

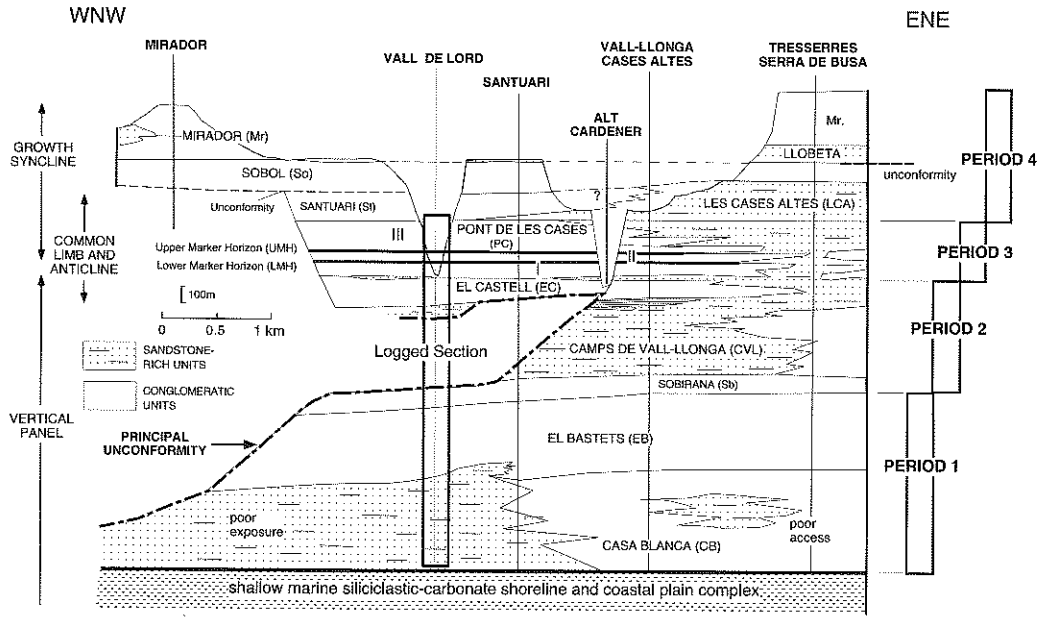

Fig. 2. Diagram showing lithostratigraphical units and the main unconformities of the Berga Conglomerate Group near Sant Llorenç de Morunys, and the relationship to Periods 1–4 defined by stratigraphical architecture. The general location of the logged section in the Vall de Lord is boxed.

angular unconformity (Fig. 6a) which becomes bedding-parallel toward the south. This is the principal growth unconformity (see also Fig. 2 and Riba 1976*b*). The growth fold pair is clearly visible in younger strata to the south (Fig. 6b) and can be traced eastward into the Tossal de Vall-llonga on profile 2 as can the principal growth unconformity (Fig. 5b). East of Vall-llonga (the next valley to the east), only the growth syncline is clearly visible (profile 3, Fig. 5c) and there is a gradual transition from overturned beds southward into flat-lying beds. The significant along-strike variations in growth strata history partly correlate with an eastward increase in fold size.

Structural orientation data for the whole region (Fig. 4) give a mean sub-horizontal fold axis trending 1°–284°; minor local variations in fold plunge are detailed in the three-dimensional structural analysis of Ford *et al.* (1997). The asymmetrical fold pair comprises an anticline whose axial surface can be continuous or fragmented into en-echelon segments and which overall shows either a shallow hinterland, or sub-horizontal sheet-dip, and a syncline whose curved axial surface has a moderate hinterland dip (Figs 5 & 6b). The generalized fold axial surfaces converge upwards. However they do not meet at a point, but become parallel or die out in the highest strata (Fig. 6b). Principal and subsidiary angular unconformities are developed in the growth anticline and upper parts of the common limb, while composite offlap-onlap is observed in the growth syncline. Major thickness changes occur across the anticlinal and synclinal axial surfaces and across the common limb. Dips shallow upward into younger beds within the common limb. An anticlockwise axially transecting cleavage exists in sandstones of the growth syncline hinge region. Minor thrusts and strike-slip faults record brittle down-dip and along-strike extension in steep strata.

Based on these observations and sequential restoration of three cross sections (Fig. 5), it was concluded by Ford *et al.* (1997) that the fold pair grew principally by progressive rotation of the common limb and that folding was ongoing at all levels of the structure. Deposition of wedge-shaped units of sediment across the growing fold pair forced the limb to lengthen with time. The fold is considered to have developed ahead of a propagating low-angle blind thrust (i.e. a fault propagation fold; Fig. 1c), the position of the tip of which is unknown. Suppe *et al.* (1997) present an alternative interpretation for the upper 500 m

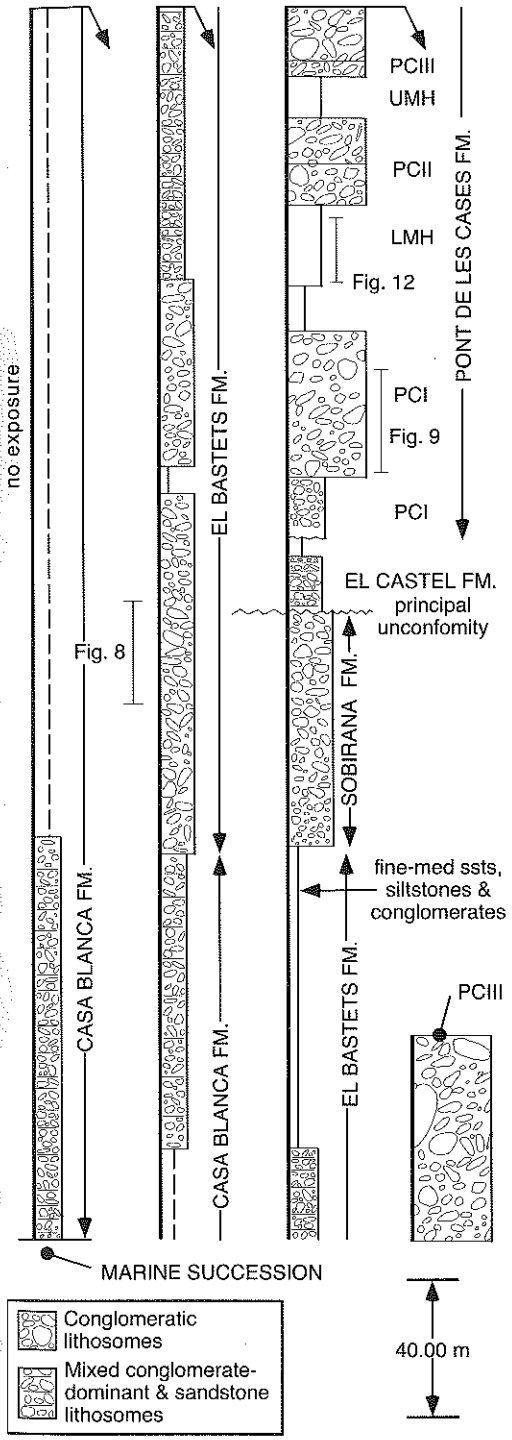

Fig. 3. Simplified vertical stratigraphic section, exposed along the Cami del Santuari (Vall de Lord, see Figs 2 and 4 for location), from the marine-continental boundary to base of the Les Cases Altes Formation.

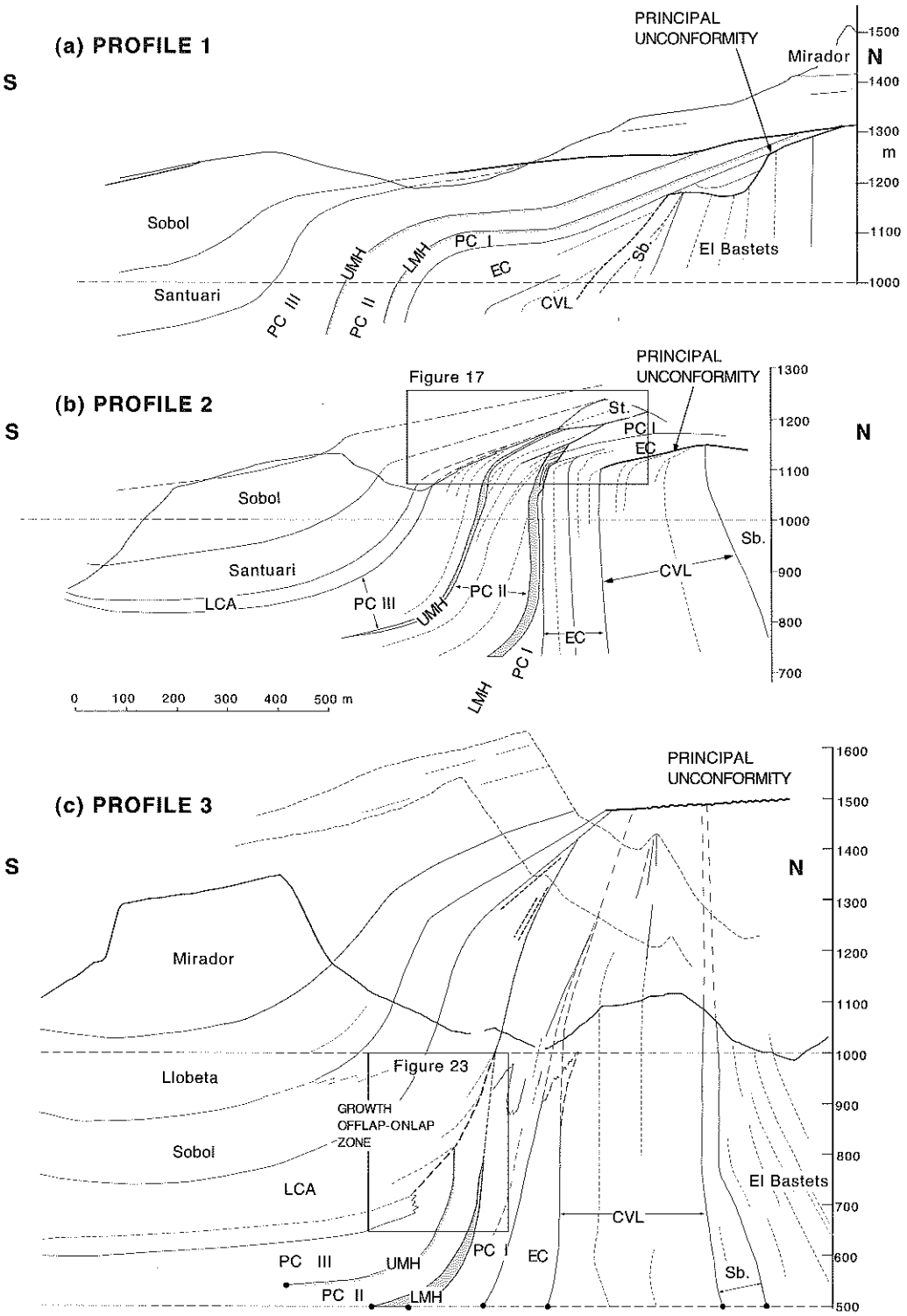

Fig. 5. Three dip-parallel cross-sections across the Sant Llorenç growth structure, located in Fig. 4 (modified slightly from Ford *et al.* 1997, fig. 19). Abbreviations for stratigraphical units as in Fig. 2

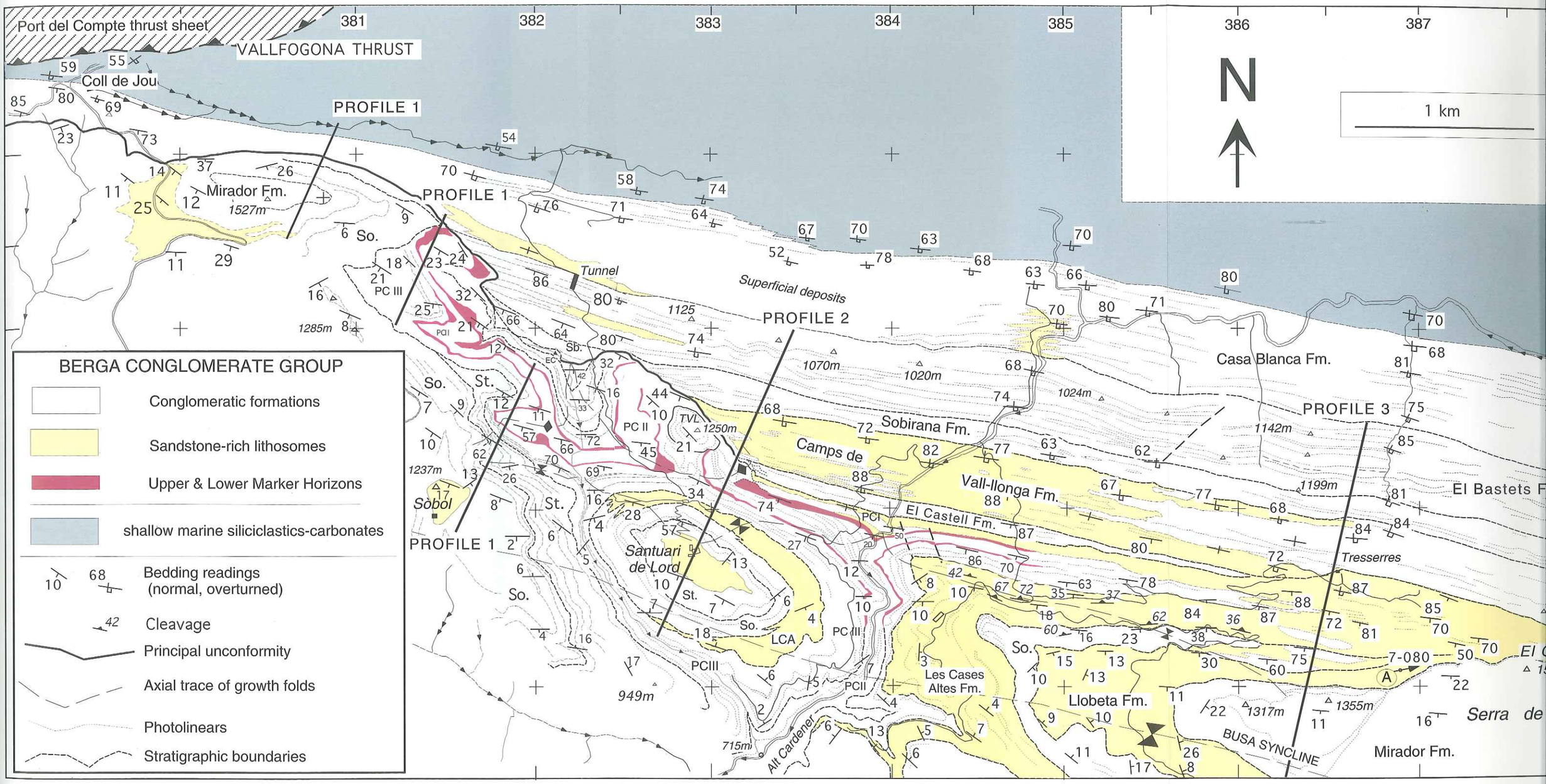

Fig. 4. Simplified geological map of the Sant Llorenç de Morunys growth structure, showing the locations of profiles 1–3 (see Figure 5) (modified slightly from Ford *et al.* 1997, fig. 5).

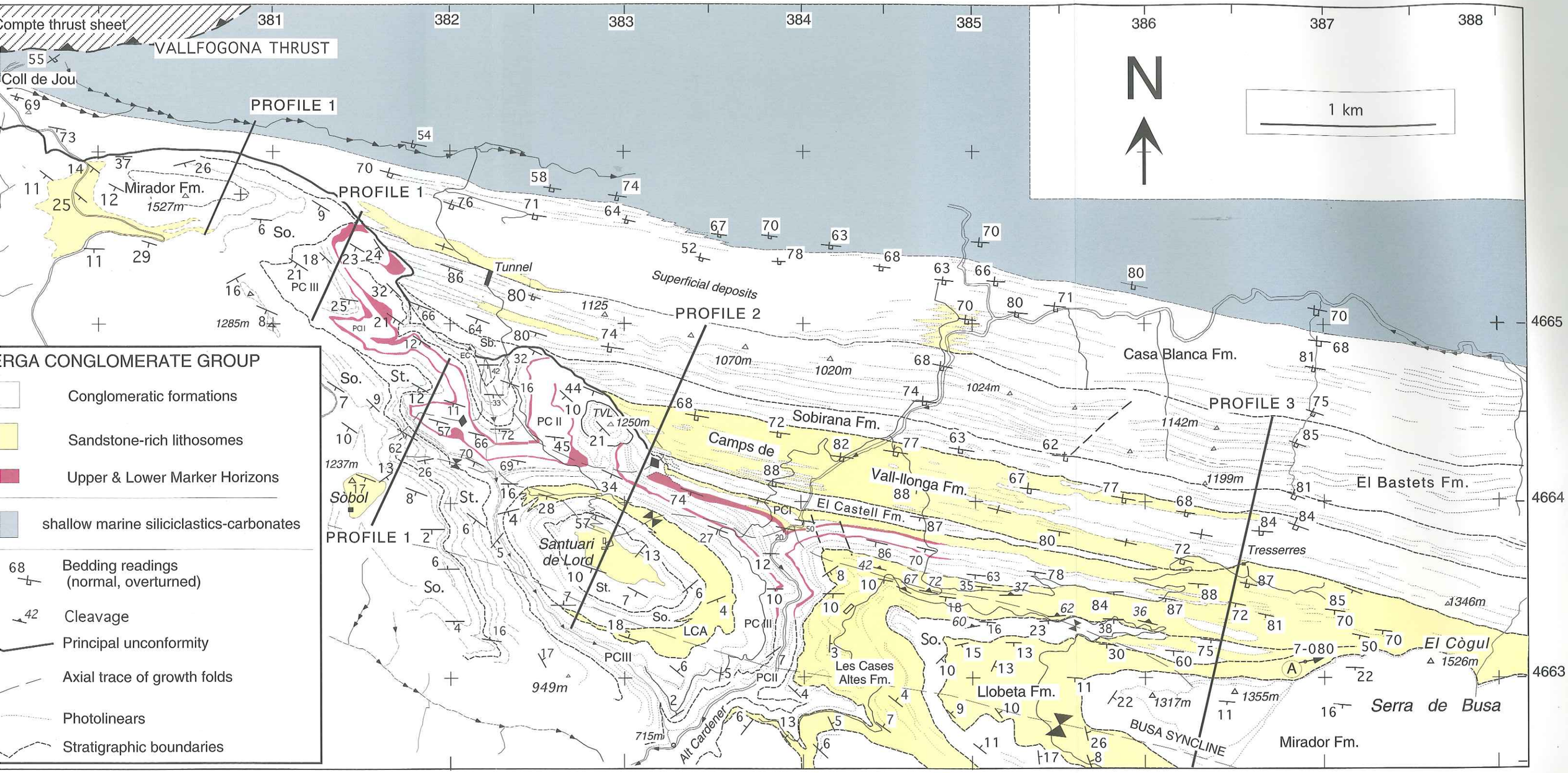

d geological map of the Sant Llorenç de Morunys growth structure, showing the locations of profiles 1–3 (see Figure 5) (modified slightly from Ford *et*

(a)

(b)

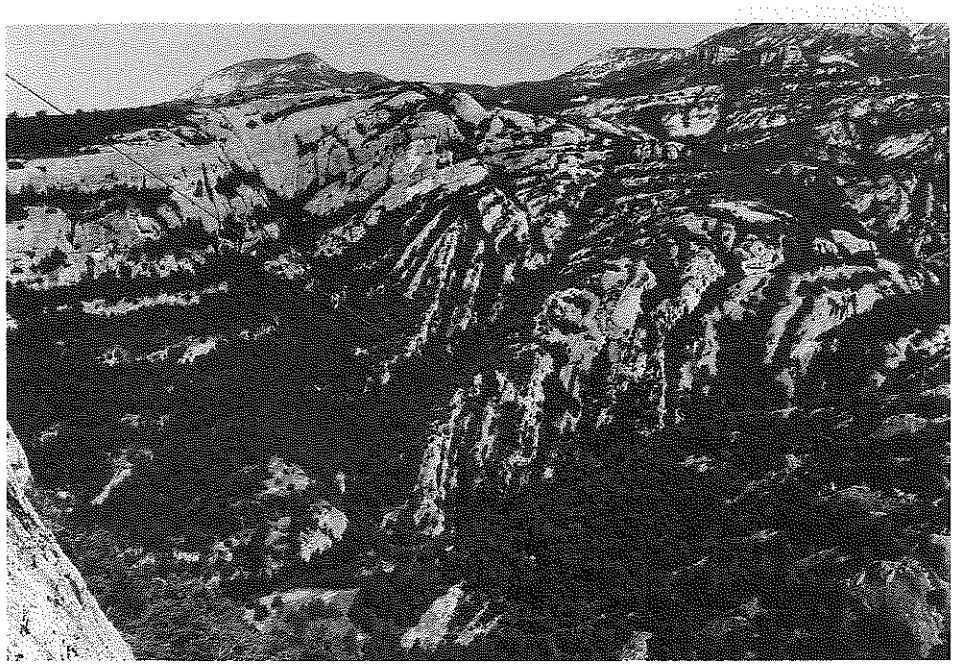

Fig. 6. (**a**) Photograph (view to the west) of the principal unconformity as depicted on profile 1, in an approximately dip-parallel section. Vertical to overturned conglomerate beds of the El Bastets and Sobirana Formations showing a continuous spectrum of dips until truncated by the unconformity. The highest, gently-dipping beds are of the Sobol and Mirador Conglomerate Formations. (**b**) Photograph of an oblique view of the section depicted in profile 1 on the west side of Vall de Lord, illustrating the thickening of stratigraphical units across the growth anticline, and the rounded hinge forms of the anticline and syncline. In the middle ground are flat-lying conglomerates above the principal unconformity up to the Mirador Formation. In the background to the right are the Eocene carbonates of the Port del Compte thrust sheet.

of the growth fold, arguing that it developed by curved-hinge kink-band migration predicted by the fault-bend fold mechanism, which caused lengthening of the common limb but no limb rotation.

Sedimentology

The purpose of this section is to establish the *basic* emplacement processes of the volumetrically dominant (modal) conglomerate and sandstone facies that make up the growth strata at Sant Llorenç de Morunys, in order to understand the relationship between surface processes and deformation. The sedimentological analysis is centred on a well exposed road section in Vall de Lord (Fig. 4) which cuts obliquely across the growth fold pair, including conglomerates of the vertical panel, and thus samples several geometrically complex lithosomes. With only one large exposure gap (Fig. 3) the section extends from the conformable contact with marine strata to the base of the Les Cases Altes Formation (Figs 2 & 3). Approximately 700 m of this section were logged on a bed-by-bed basis at a scale of 1:25; this database was supplemented by observations and measurements from other well exposed regions of the growth structure. Data collected for each bed included size/frequency of framework clast modes, framework clast shape and roundness, percentage and type of matrix, clast support system and fabric type. Details of the bed geometry, structures and stratification were routinely recorded. Clast size-bed thickness and palaeocurrent analyses were also carried out, the details of which are given below.

Formation and member divisions of the Berga Conglomerate Group have been principally established on the basis of proportions of three broad lithologies: granule to small boulder conglomerates, lithic arenites and pebbly (lithic) sandstones. The latter pair tend to vary inversely in occurrence with the more varied conglomerate facies. Siltstone lithologies are comparatively rare, tending to occur in overall finer-grained formations. Detailed information regarding the clast populations of the conglomerates will be given elsewhere. In general, however, typical beds are polymict, with varied carbonate rock types predominating. As noted by Riba (1976*b*) clasts of acid–intermediate plutonic rocks, Permo-Triassic red beds, Carboniferous micro-conglomerates, rare metasedimentary rocks and basic igneous rocks indicate that drainage basins extended (or were linked) to the Pyrenean axial zone where basement rocks outcrop. The large volumes of varied, generally fine-grained, carbonate rock types reflect significant source areas in the Mesozoic–Cenozoic sequences of the south Pyrenean thrust sheets (Fig. 1b). No major difference in roundness or mean shape is noticeable between clast types of clear axial zone origin or those from the less distant thrust sheets, although roundness is greater for axial zone clasts. In general, more petromict assemblages appear at the top of the Casa Blanca Formation, and persist with significant internal variations until mid levels of the Mirador Formation (Fig. 2), where assemblages are very enriched in limestone and sandstone clast types. Signatures of radically different provenances within the succession, however, have not been detected.

Conglomerate facies

The conglomerates (Fig. 7) are split into two broad categories: (1) unstratified, coarse-grained, matrix-rich conglomerates, which form the modal conglomerate type and (2) variably stratified conglomerates, with varied matrix type and proportion. All facies categories have been analysed in terms of their bed thickness (B.Th) and clast size characteristics, following the methods of Bluck (1967) and Nemec & Steel (1984). The mean maximum particle size (MMPS) for individual beds was obtained by measurement of the *a* (long) axis of the ten largest clasts restricted to a 2 m wide zone about the point of observation. In the case of very thick (>1 m) beds, the ten largest clasts were recorded for uniform divisions of the bed in order to eliminate underestimates of the largest clasts, and to establish or verify any coarse tail grading profile. Any clear outsize clasts were noted, and separate MMPS plots prepared. The scatter plots presented are in a similar form to those of Nemec & Steel (1984, fig. 19) in order to facilitate comparisons with the flow competence–thickness models they discuss.

Unstratified, coarse matrix-rich conglomerates. This category forms the volumetric bulk of the conglomerates, and has been analysed initially without further subdivision on the basis of grading type (see below). Characteristically, unstratified conglomerates occur in beds up to 1.75 m thick, though exceptionally up to 6 m. Beds are dominantly unordered, with modal framework grains of rounded to well-rounded large pebble to small cobble size, often characterized by distinct polymodal distributions (Fig. 7a). The matrix is typically coarse-grained sand to small pebbles, with occasional prominent admixtures of orange-red fine–medium silt, or rarer medium grey calcareous mud. The matrix

is frequently rich enough to locally support the framework clasts, most commonly allowing point contacts, and coarse matrix-supported facies are commonly noted (Fig. 8). The polymodal nature frequently makes difficult the distinction between matrix and framework. Clast fabrics, where developed, are most commonly *a*(p)*a*(i) imbrication, which tends to be a 'dispersed' rather than a pervasive fabric (Fig. 7b), or *a*(p)*a*(i) clast nests (Allen 1981). Well developed sub-horizontal, bedding-parallel alignment of *ab* planes is rare; unstratified conglomerates are much more likely to be chaotically-organized with frequent examples of large cobbles or

(a)

(b)

(c)

(d)

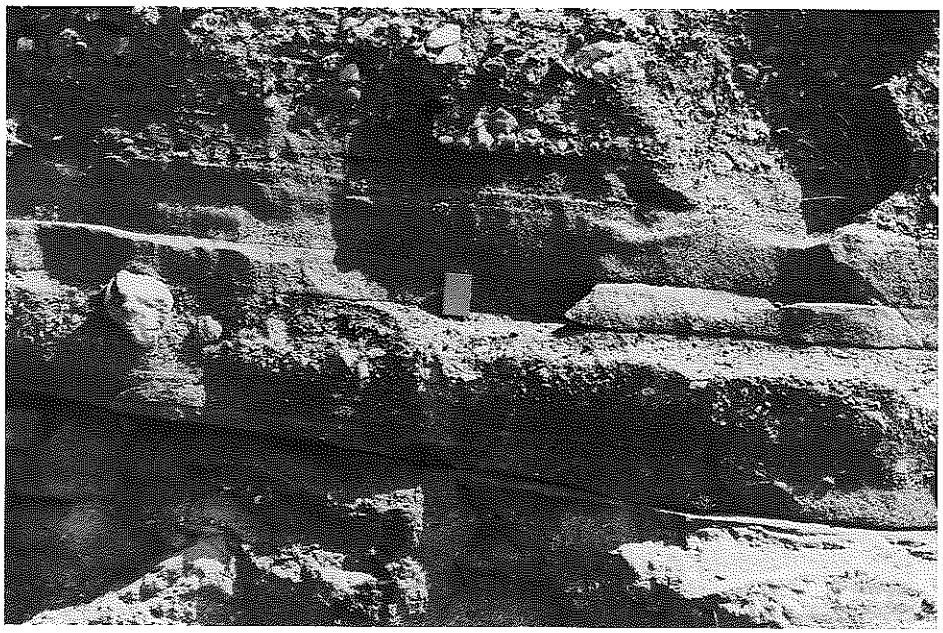

Fig. 7. Photographs showing the texture and fabric of the main conglomerate and sandstone facies. (**a**) Typical unstratified, large cobble to boulder grade conglomerate. Scale ruler is 0.4 m long. (**b**) Moderately-developed *a*(p)*a*(i) imbrication fabric of the unstratified conglomerate facies. Ruler scaled in cm, visible length is 0.22 m. (**c**) Fine matrix-supported medium-large pebble conglomerate (cohesive debris flow), in which orange silt matrix becomes dominant upwards. Top is truncated by a sharp erosional basal surface of the overlying pebble-cobble conglomerate. Member I of the Pont de les Cases Formation. (**d**) Sequence of generally small pebble-grade sheet-like, stratified clast-supported and matrix-supported conglomerates from the lower marker horizon (see Fig. 12), from *c.* 84–87 m. Notebook is 0.2 m long. (**e**) Draping coarse-grained, granule-very small pebble bearing sandstone, overlying a clast-supported, well-imbricated (probably *a*(t)*b*(i) type) pebble- to large cobble-grade conglomerate.

(e)

small boulders with steep or vertical *ab* planes. Fabric development is not thought to be controlled by the availability of discoidal or bladed clasts; such shapes are readily found in all of the coarse conglomerate facies, and are not preferentially sorted as part of lateral facies assemblages of the type generated by processes operating on gravel river bars (e.g. Bluck 1976; Haughton 1989). Rare outsized clasts are frequently concentrated at the top or upper part of beds. A small proportion of unstratified conglomerates display poorly–moderately developed *a*(t)*b*(i) fabrics and clast clusters (Brayshaw 1984), and tend to show better clast support systems (Figs 7e & 9).

Unstratified conglomerate beds have flat–sharp and sharp–irregular erosional bases (Fig. 7c), and tend to be sheet-like at the scale of exposure. Basal surfaces are also characterized by erosional longitudinal scours. Conglomerate sheets frequently show steep to vertical erosional margins, less often low-angle (concave-type) channel margins, and equally rarely transitional–gradational contacts to other (finer-grained) facies. Relief on steep margins is frequently of the order of the bed thickness, but may be several metres in rare cases.

A plot of MMPS against B.Th for unstratified conglomerates shows moderate positive linear regression (Fig. 10a), with increasing scatter of the data at higher values of both parameters. The distribution indicates a low value positive *y* axis intercept, which closely approaches the origin. Plots of the *maximum* clast size versus B.Th give similar results. The very high correlation of MMPS and maximum clast size in beds ($r = 0.94$–0.952, Fig. 10b) points to a lack of outsized clasts; a nearly identical relationship for similar alluvial conglomerate facies was interpreted by Nemec *et al.* (1984) to indicate efficient sorting of the framework clast population. Sorting of the coarse tail component, however, appears to decrease with increasing grain size (Fig. 10c).

Interpretation. The conjunction of significant positive correlations between bed thickness and both MMPS and maximum clast size, with matrix-supported textures, occasional parallel imbrication but largely unordered fabrics suggests a mass flow origin for the bulk of these conglomerates (Bluck 1967; Nemec & Steel 1984). The absence of silt- or clay-rich material in the matrix of the majority of unstratified conglomerates and the trend for data points to pass through the origin of a MMPS:B.Th plot further suggests that the deposits were emplaced as density-modified grain flows (Lowe 1976), equivalent to the cohesionless debris flows of Nemec & Steel (1984). Separate analyses of the small number of clast-supported unstratified conglomerates also show similar positive correlations, and thus imply comparable emplacement mechanisms operated. The highly

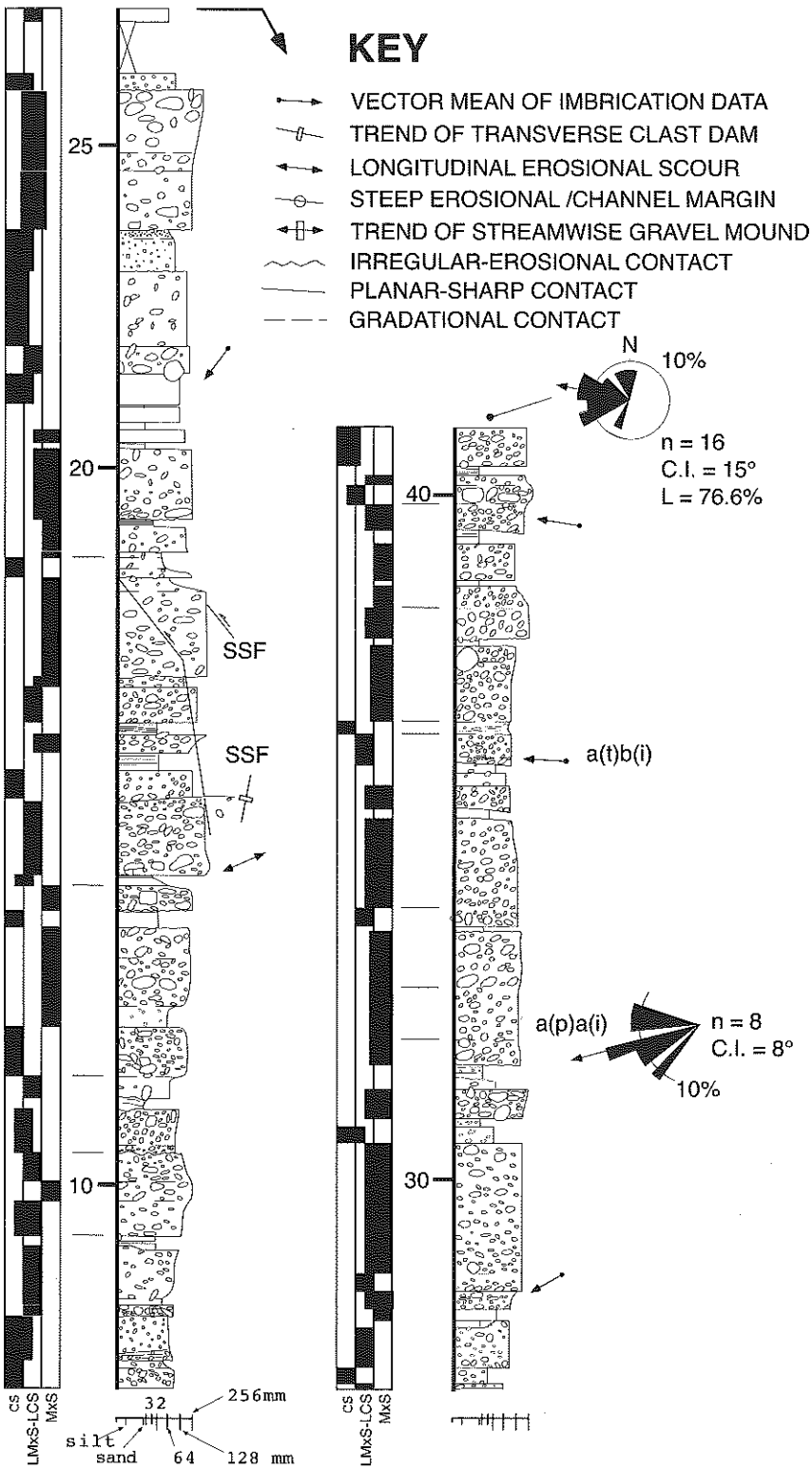
KEY
VECTOR MEAN OF IMBRICATION DATA
TREND OF TRANSVERSE CLAST DAM
LONGITUDINAL EROSIONAL SCOUR
STEEP EROSIONAL /CHANNEL MARGIN
TREND OF STREAMWISE GRAVEL MOUND
IRREGULAR-EROSIONAL CONTACT
PLANAR-SHARP CONTACT
GRADATIONAL CONTACT
N
10%
n = 16
C.I. = 15°
L = 76.6%
25
20
10
40
30
SSF
SSF
a(t)b(i)
a(p)a(i)
n = 8
C.I. = 8°
10%
cs
LMxS-LCS
MxS
silt
sand
64
32
128 mm
256mm

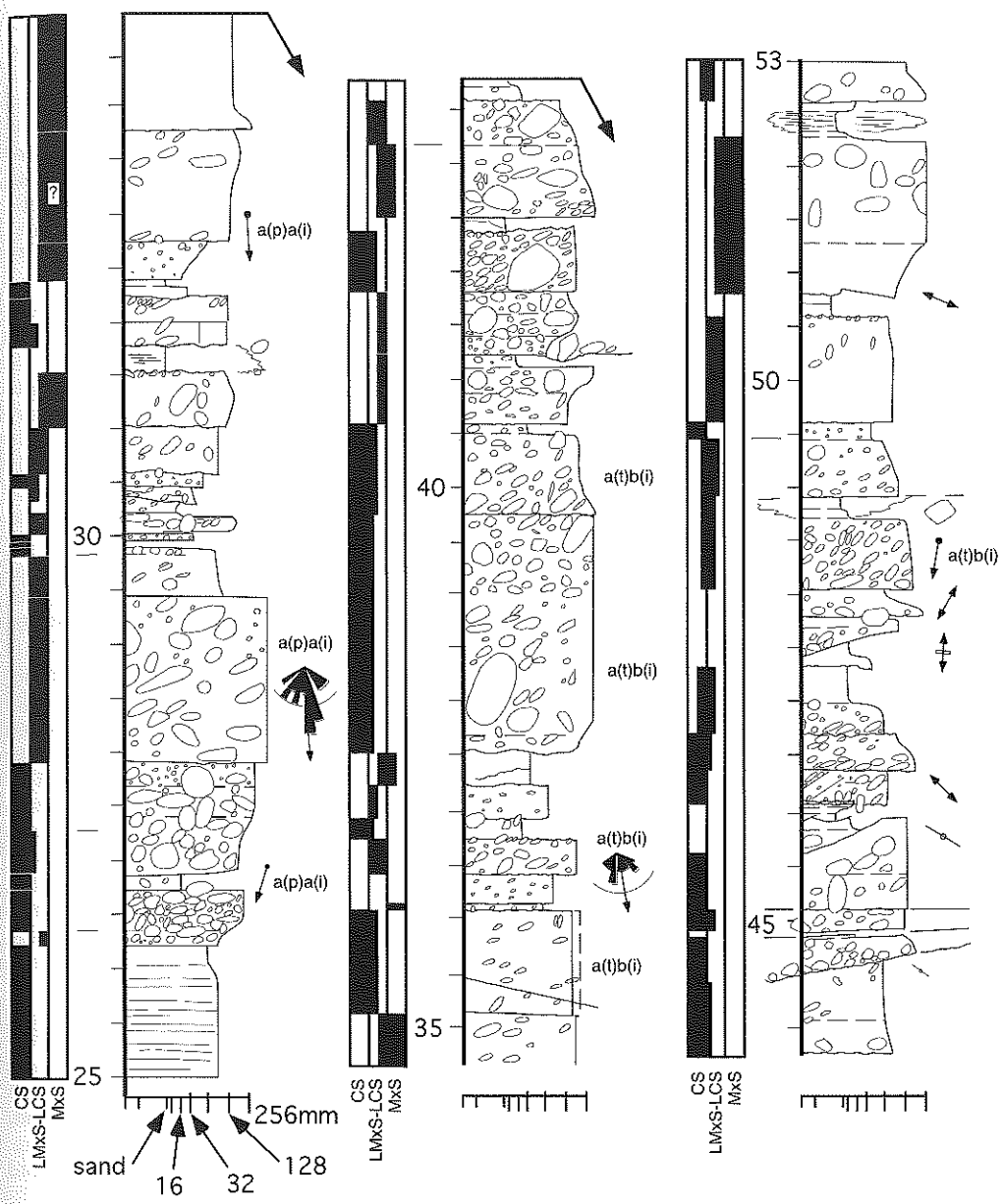

Fig. 9. Graphic log detailing conglomerate facies in member I of the Pont de les Cases Formation. This coarse-grained section above the principal unconformity of the growth structure, contains unstratified, polymodal, coarse matrix-rich conglomerates, which show a suite of grading profiles. Several examples of matrix- to local matrix-supported *a*(p)*a*(i) imbricated large cobble to small boulder grade conglomerates. Rose diagrams for imbrication data show vector mean arrow, and the radius of the arc indicates 10% of points.

Fig. 8. Detailed graphic log of characteristic conglomerate facies from the El Bastets Conglomerate Formation (of Period 1). See Fig. 3 for location. Vertical scale for all logs in metres. Filled areas of the left hand columns indicate the clast support system for each bed, where CS is clast-supported, LMxS-LCS is local matrix support to local clast support, and MxS is matrix-supported. The matrix in this section is almost invariably in the range from medium-grained sand to small pebbles. North for palaeocurrents is to the top of the page. Note the pair of minor syn-sedimentary contraction faults (SSF) cutting conglomerate beds at 15–18 m.

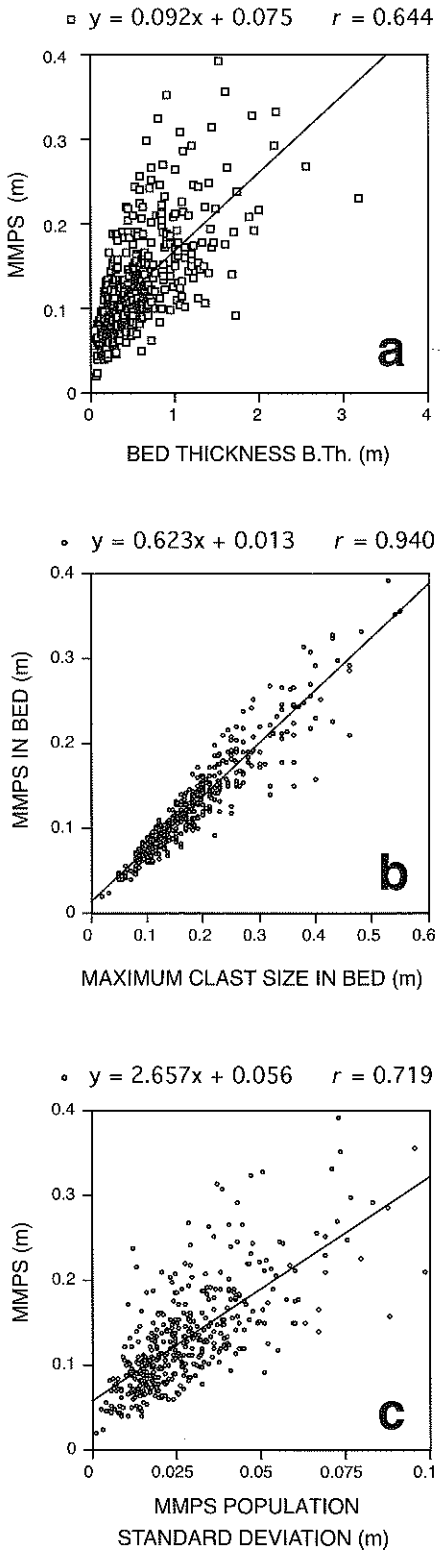

extensive, frequently erosionally based and fine-matrix-poor nature of the gravels imply that these were during single, variable magnitude flood events, rather than typical sediment gravity flows (Blair & McPherson 1994*a*).

Sub-division of unstratified, matrix-rich conglomerates into grading types (e.g. Nemec *et al.* 1984) has been carried out, and the results plotted in Fig. 11 using the maximum particle-size parameter. This can be used in place of MMPS because of the high correlation between the two parameters (Fig. 10b). Ungraded conglomerates form the largest sub-group ($n = 174$), and show a moderate positive linear correlation (Fig. 11). Separate analyses of unstratified conglomerate categories of different grading profile (top-only normally-graded, inversely-graded, base-only inversely graded, and inversely to normally graded types) all give significant positive linear correlations with r values ranging from 0.64 to 0.73 for different ranges of grain size. These types are generally considered the result of cohesionless mass flows (cf. Allen 1981; Nemec & Steel 1984). The MMPS:B.Th relationship of unstratified normally graded conglomerates ($n = 112$) is considerably less well correlated. This probably reflects the inclusion of polymodal clast-supported (relatively matrix poor) beds, with dispersed type *a*(t)*b*(i) fabrics, in the analysis. These are likely to result from bed load transport in stream flows (e.g. Allen 1981; Steel & Thompson 1983). A relatively small population of silt–sand matrix-supported, massive conglomerates have been included in the data analysis summarized in Fig. 11. The poorly sorted texture, chaotic fabric tendency (Fig. 7c) and capability of supporting outsize clasts (e.g. Fig. 12 at 93 m) suggest that these are cohesive (viscous) debris flows.

The particle size–bed thickness data presented in Fig. 11 is broken down into information (a) from Period 1 (Fig. 11a) of the growth structure evolution (structurally beneath the principal unconformity in the measured section, Figs 2 & 4a), and (b) from Periods 2 and 3 (Fig. 11b), from rocks associated with the growth fold

Fig. 10. (**a**) Scatter plot of mean maximum particle size (MMPS) versus bed thickness (B.Th) for the unstratified conglomerate facies up to bed thicknesses of *c.* 3 m, showing regression equation and correlation coefficient (r). Rare cases of thicker beds (up to *c.* 6 m) have not been included but give a similar correlation ($y = 0.099x + 0.071$, $r = 0.729$). (**b**) Plot of maximum particle size against mean maximum particle size in all unstratified conglomerate beds. (**c**) Plot of mean maximum particle size against population standard deviation of the MMPS for the same facies.

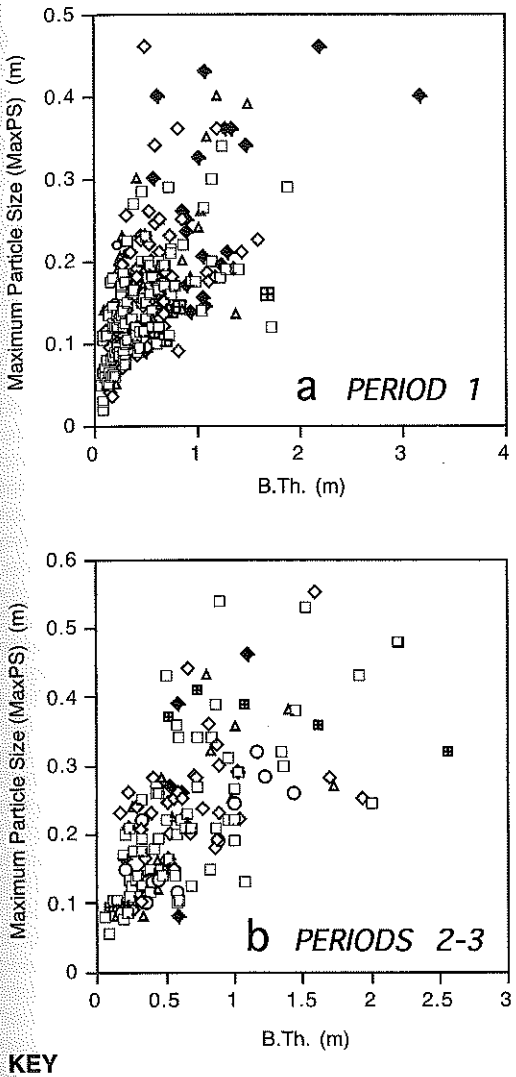

Fig. 11. Plots of maximum particle size (MaxPS) against bed thickness (B.Th.) for the unstratified conglomerate facies sub-divided by grading profile for (**a**) beds of Period 1 within the vertical panel beneath the principal unconformity ($n = 275$), and (**b**) beds of Periods 2 and 3 from the common limb and anticline of the growth structure ($n = 145$). Both show well-developed positive correlations, suggesting similar emplacement mechanisms operated for conglomerates of the vertical panel, and those above the principal unconformity.

pair. This is in order to test whether apparently similar conglomerate facies had similar flow competence-thickness relationships (and magnitudes) when deposited in different regions of the palaeosurface affected by the growth structure, possibly under the influence of contrasting syn-depositional surface deformation. The similar distributions revealed (Fig. 11a, b) suggest that the same emplacement mechanisms operated during Period 1 as in later periods for which there is data, arguing that there was a continuity of processes (and probably environmental conditions) throughout the history of the structure.

Stratified and sand-rich conglomerates. Of this category, the most important representatives are horizontally stratified, and (low-angle) inclined stratified conglomerates, both of which tend to be clast-supported and normally- to un-graded (Figs 7d, 9 & 12). The horizontally stratified facies tend to show basal lags of large pebbles and cobbles above irregular-sharp erosive surfaces, in beds of typical thickness range 0.2–1.5 m. Low-angle (inclined) stratified conglomerates are often heterolithic, in containing lenses or layers of pebbly sandstone, and also show *ab* planes of bladed clasts sub-parallel to the inclined layering. Evidence of 'lateral accretion', from the parallel directions of basal erosional structures and the strike of inclined layering is evident in a number of examples. Both facies are transitional to sand-rich (pebbly) conglomerates, which may be flat-bedded, contain inclined strata or structureless. Large-scale cross-stratified conglomerate facies are very rare throughout the succession.

Interpretation. Horizontally stratified conglomerates are interpreted as the product of rolling of bedload beneath stream flows. The sand-rich gradational version of this facies probably involved the simultaneous transport in suspension of relatively fine gravel and coarse sand. Conglomerates with inclined stratification indicate the existence of significant depositional relief in local sub-environments, and probably represent the flanks of longitudinal bars. A similar designation can be made to the horizontally stratified conglomerates, which would constitute the low-angle bar tail region (Hein & Walker 1977; Nemec & Postma 1993), although lateral facies transitions do not reveal bar head conglomerate facies.

Sandstone facies

Sandstones occur in three associations: (i) as thin (<0.6 m), typically laterally impersistent

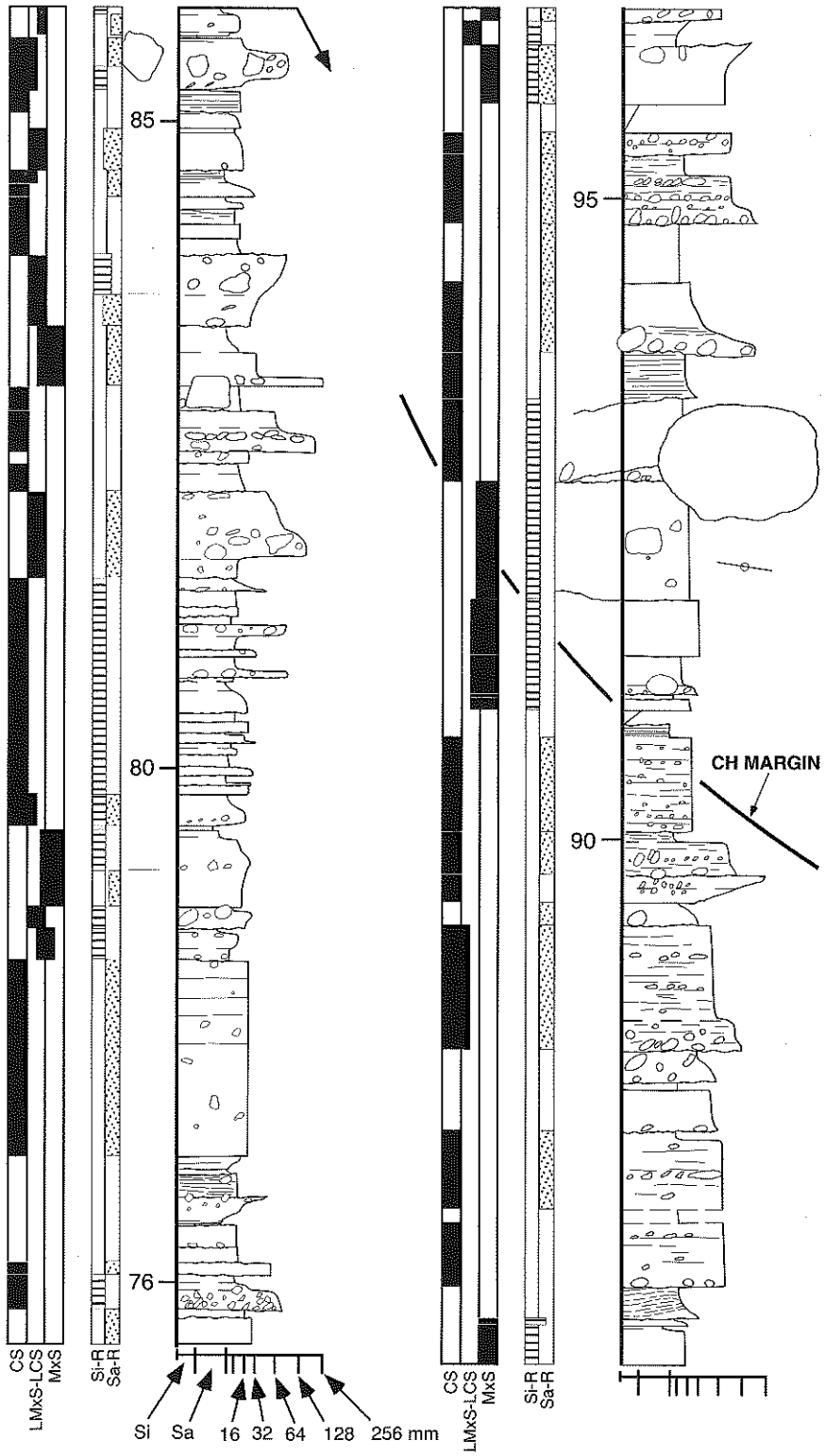
85
80
76
95
90
CH MARGIN
CS
LMxS-LCS
MxS
Si-R
Sa-R
Si
Sa
16
32
64
128
256 mm

gradational caps on conglomerate beds, (ii) as decimetre- to metre-scale bedsets, associated with siltstone and sandy conglomerate facies, and (iii) reddened silt-rich sandstones laterally-equivalent to fine matrix-supported conglomerates.

Sandstones are typically medium to very coarse grained, and frequently contain dispersed ('floating') granules and small-medium pebbles, which may also be concentrated in impersistent layers. Those occurring as conglomerate caps (Figs 8 & 9) tend to be coarser grained and fine-gravel bearing (Fig. 7e). This type is frequently horizontally parallel-laminated, but forms a continuum to three-dimensional non-parallel undulatory–sinusoidal stratification, observed in rare cases as lateral transitions. Sinusoidal–undulatory sandstones may incorporate solitary outsize (cobble-grade) clasts, and thin lenses of fine pebbly gravel. Occasionally, primary convex-upward tops, and isolated domes or hummocks above conglomerates are preserved. This sub-facies clear connection with often normally graded, clast-supported conglomerates suggests emplacement from standing wave-antidune type bedforms in supercritical flows, and shallowing high velocity flows, to give parallel-laminated and massive beds. In this connection it is notable that very few of the sandstones transitional from conglomerates throughout the succession are (large-scale) cross-stratified as has been commonly reported in other successions (e.g. Allen 1981; Todd 1989).

Medium–fine-grained sandstones occurring in thick packages are massive to horizontally planar parallel laminated. They are commonly highly reddened, and show evidence of strong bioturbation by *?planolites*- and *cylindricum*-type burrowers, and unidentified grazers. These sandstones are interpreted as the product of shallow unconfined flood events, which accumulated in regions bypassed by major gravel input. The third association of distinctive silt-rich sandstone facies contains floating, unordered gravel clasts, and has highly irregular, gradational contacts to conglomerate beds, and clearly suggests cohesive sandy ('clast-poor') debris flows.

Siltstone facies

This volumetrically rare facies occurs as two contrasting sub-facies: (i) structureless or blocky red-orange siltstones, in thick (metre-scale units) or very thin 'drapes' and (ii) poorly-sorted sand- (and more rarely granule-) bearing siltstones, associated with other fine matrix-bearing or matrix-supported sandstones and conglomerates. Sub-facies (i) is interpreted as repeated suspension-deposit events, subsequently weakly pedogenically modified. This is in frequent association with medium–fine-grained parallel-laminated sandstones, organized in thick (metre-scale) units of alternating facies. Sub-facies (ii) is considered to represent viscous mud flows, the dominant silt matrix having the strength to support sand and very fine gravel.

Palaeocurrents

Sediment dispersal within the system was investigated by the measurement of a suite of primary structures considered to represent flood-stage palaeoflow. The most common structures for which palaeocurrent directions were determined were longitudinal erosional scours on conglomerate bases, steep margins of conglomerate beds, incised channel margins, conglomerate clast imbrication, clast *a*-axis alignment, obstacle scours, cross-stratification, and primary current lineation in sandstones. Because of the complex and systematically varying bedding orientations intrinsic to the Sant Llorenç de Morunys growth structure, data were individually stereographically restored to horizontal using locally collected bedding data. Corrections for the variably oriented fold axes were not performed because of the low (1–5°) plunge values for sub-areas of the structure (Ford *et al.* 1997). Derivation of palaeocurrents from conglomerate fabrics involved direct measurement of *ab* planes and *a* axes of representative bladed–discoidal clasts in single beds. Following structural restoration, the inferred palaeoflow direction for each clast was determined by the dip-azimuth of *ab* + 180° and the vector mean and magnitude of the sample calculated. Rayleigh tests were routinely applied, and vector means rejected if the test was failed at the $p = 0.05$ level of significance (Curray 1956). The spatial relationship of *ab* and *a* was stereographically assessed, following restoration, to distinguish *a*(p)*a*(i) and *a*(t)*b*(i) type fabrics. Palaeoflow from the preferred orientation of clast *a*-axes, was

Fig. 12. Detailed graphic log of the lower-mid section of the lower marker horizon (Pont de les Cases Formation). This horizon contains a mixture of (i) small-medium pebble, thinly-bedded horizontally-stratified conglomerates with sub-angular framework clasts, and (ii) fine-grained granule to pebble, silt matrix-rich to matrix-supported conglomerates. Filled areas of the far left hand columns indicate the clast support system (abbreviations as for Fig. 8), and ornamented areas of the central columns specify the predominant matrix type, Si-R, red-orange coloured silt/mud-rich; Sa-R, sand- (plus granule–very small pebble gravel-) rich.

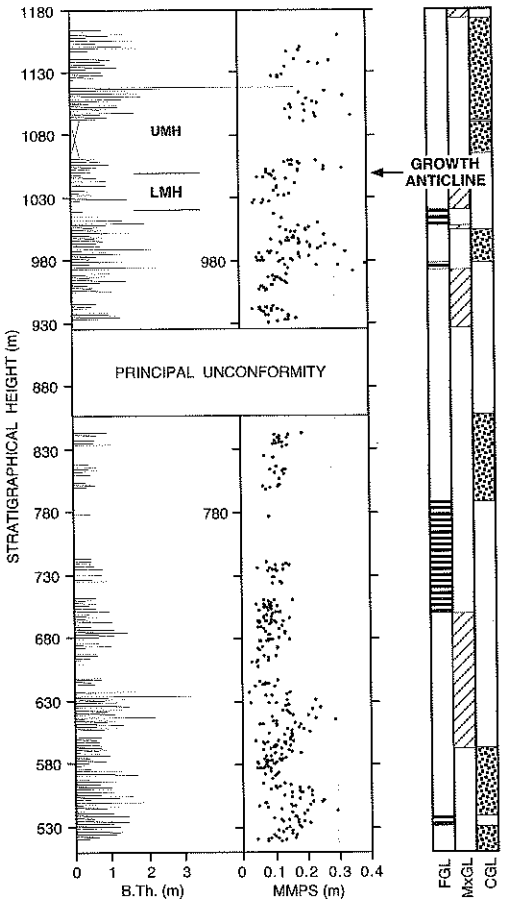

Fig. 13. Combined bar graph of bed thickness (B.Th) and plot of mean maximum grain size (MMPS) against stratigraphical height for the principal logged section in Vall de Lord (Fig. 3). Broken lines in the bar graph denote individual bed thicknesses at similar stratigraphical levels not resolvable at this scale. Also shown are positions of the principal unconformity, position of the growth anticline axial surface in the section, and the Upper and Lower Marker Horizons. Right hand columns characterize the bulk grain size of the lithosomes represented in the section: FGL, fine-grained; MxGL, mixed grain size, and CGL, coarse-grained (conglomeratic) lithosome.

determined using measurements made in the bedding plane.

Data were collected from a large area of the structure. Much information is derived from the principal logged section, spanning the region between profiles 1 and 2 (Fig. 4), whereas a more areally spread dataset exists in the region between profiles 2 and 3 from the trace of the Busa Syncline northwards to the El Bastets Formation outcrop (Fig. 4). Information is thus common, in the west of the structure, in association with the steep panel and growth anticline, whereas in the east it applies mainly to the growth syncline and to the steep common limb (Fig. 5c). It is thus currently not viable to compare palaeoflow in different limbs of the growth fold pair *directly* across strike, but this can be done for the structure as a whole.

Examples of the local variability of palaeoflow in relation to facies units and structures are shown in Figs 8 and 9. Palaeoflow in these cases remained consistent over vertical intervals of 10–25 m. No systematic switching of palaeocurrents (e.g. Haughton 1989, fig. 8) is clearly evident between stacked facies units, or in rare gradationally bounded conglomerate packages. The texture, facies structure and organization of the conglomerates (see above) are unlike those of low-sinuosity, gravel-bed permanent rivers in which palaeocurrents are frequently at high angles to the channel direction (regional palaeoslope; Bluck 1976, figs 19 & 20), suggesting that differing palaeocurrent modes (see below) do reflect differing palaeoslopes within the growth structure.

Grain-size variations

Details of the vertical variation in conglomerate bed thickness and corresponding data on the mean maximum clast size are shown in Fig. 13. Vertical cycles based on grain size (MMPS) are not clearly developed on the scale of succession illustrated (El Bastets to Pont de les Cases Formations). Intervals of *c.* 100 m show neutral trends in MMPS, and are not always affected by boundaries of formational (or lower-order) lithosomes of contrasting grain size. However the obliquity of the measured section with respect to the geometrically complex lithosomes partly accounts for the complexity of the vertical trends. A major increase in MMPS and a corresponding increase in bed thickness occurs approximately 50 m above the principal unconformity (Fig. 13). This abrupt increase is not compatible with definition of a gradational coarsening-upward megasequence; indeed organized sequences of this scale are not immediately clear from the successions preserved in the growth structure. The effects of the principal unconformity on laterally equivalent and overlying conglomerates were limited due to the restricted time span over which it operated within the growth structure. It is therefore not thought to be responsible for recycling

proximal facies to build medial and distal parts of lithosomes on a significant scale. Analysis of the grain size data on a smaller scale reveals neutral, upward-coarsening and upward-fining cycles of variable thicknesses ranging from 6.5 to 25 m. These are broadly comparable in scale to the sequences, small-scale cycles and fifth-order lithosomes respectively of Heward (1978, fig. 11), Gloppen & Steel (1981, fig. 17) and DeCelles *et al.* (1991*a*, figs 2 & 12), although not in detailed facies organization. These are interpreted as alluvial fan-trench (incised fan-channel) deposits (Heward 1978; DeCelles *et al.* 1991*a*) and progradational fan-lobe deposits (Gloppen & Steel 1981).

The restricted horizontal extent of the measured section in growth strata above the principal unconformity does not allow specification of trends in lateral grain size variation. Therefore it is not currently possible to make inferences on fan scale from rates of grain-size change.

General environmental model

The modal conglomerate making up, in particular, the conglomerate-dominated lithosomes were emplaced during moderate- to high-magnitude flood events charged with high concentrations of gravel and sand (cohesionless debris flows). Associated fine-grained facies, conglomerate textures and matrix distribution imply that the majority of this conglomerate group was emplaced under sub-aerial conditions. In only a few cases where conglomerate beds show distinct upward increases in matrix volume, considered by Nemec & Steel (1984, p. 16) to indicate sub-aqueous deposition, and are associated with ephemeral lacustrine facies is this tendency excepted. The sheet-like bed geometry, laterally extensive in depositional dip and strike directions for distances of the order of 10^2 m in recent cliff and valley walls (e.g. Fig. 6a, b), suggests a frequently unconfined (sheetflood) mode of deposition. Evidence of laterally equivalent steep to sub-vertical conglomerate margins, almost certainly underestimated during data collection, indicate that the flood events had considerable erosional potential, and were in many cases emplaced as wide, but laterally confined bodies. The larger relief instances of these wide rectangular-profile channels resemble incised fan head channels (Blair & McPherson 1994*b*), and there is evidence (see below) that some existed as stable features, presumably supplying fan lobes, and were subsequently filled/buried by later sedimentation events. Inferred rectangular-profile channels scaling approximately with bed thickness are more likely to have formed simultaneously with low-frequency–high-magnitude floods, rather than have been cut during normal conditions by sediment-poor water flows. The latter are secondary fan processes (Blair & McPherson 1994*a*, *b*) forming braided-channel networks, likely to produce lower-angle erosional surfaces. Sub-aerial high viscosity (cohesive) debris flows contributed comparatively small volumes of sediment to the growth strata, and occurred more frequently during later periods of growth history. This facies is commonly associated with proximal–medial zones of steep alluvial fans (Bull 1972; Rust & Koster 1984; Blair & McPherson 1994*a*). Sandstone facies associated with the modal conglomerate type were typically deposited under upper flow regime to supercritical flow conditions. This is compatible with typical hydraulic conditions operating over alluvial fan surfaces (Blair & McPherson 1994*a*).

Stream-flow-related conglomerates are distributed throughout the succession of the growth structure, and are considered to represent a volume of the sediment that was due to relatively high-frequency–low-magnitude flow events, which may have been localized in wide-shallow channels. The sequential and textural disorganization of the several facies attributed to traction currents, and particularly the absence of large-scale cross-strata due to mesoscale bedforms or bars (*sensu* Bluck 1979) indicates that permanent, low-gradient rivers were not responsible for the alluvium accumulated in the growth structure.

The assemblage of sub-environments and processes involved suggest a type II alluvial fan setting (terminology of Blair & McPherson 1994*a*, *b*) for the sediments of the Sant Llorenç de Morunys growth structure. This fan type is defined by dominance of unconfined fluid-gravity sedimentation events, in this case characterized by cohesionless mass flows of the range discussed by Nemec & Steel (1984, fig. 15), including cohesionless debris flows and fluidal gravelly-sediment flows. Mean radial slopes of type II fans are between 2 and 8° (Blair & McPherson 1994*b*, p. 394), although a clear majority of alluvial fan types have surface inclinations of 2–5° (Blair & McPherson 1994*a*, fig. 4). Such fans (e.g. Heward 1978) are designated as 'steep', in order to distinguish them in terms of nomenclature from gravelly 'wet-type' alluvial fans (McPherson *et al.* 1987) or 'megafans', in which conglomerates are deposited in permanent (and possibly antecedent) river channel belts (Haughton 1989; Burbank *et al.* 1996). The essentially

sub-horizontal to very low-angle fan surfaces have implications for (1) the potential for deflection of palaeoflow and (2) sequential structural restoration of the growth structure. The very low-angle surfaces inferred for this environment (angles usual for depositional growth strata, Burbank *et al.* 1996) favour the deflection of palaeoflow, and in particular axial deflection, by surface perturbation caused by growth folding. Considerably greater deformation would be required to disturb transverse flows crossing steeper surfaces. As it is not possible to specify the true palaeo-depositional dip of the growth strata, it was considered valid to use the horizontal in the restorations (Ford *et al.* 1997), knowing that surficial dips were probably $\ll 5°$.

Although affected by topographic diversion due to fold growth, this proximal zone allowed large volumes of gravel to be dispersed southwards beyond the axial trace of the Puig-reig anticline (Fig. 1b). In the simplest case, involving sediment dispersal approximately perpendicular to the mountain front, this across-basin transport of gravel indicates a fan (or fans) which had a radial length of approximately 16 to 20 km. This is compatible with typical alluvial fan lengths collated by Heward (1978, fig. 3) of between 5 and 20 km, and also Blair & McPherson (1994*a*, fig. 2) who indicate a range of ≤10–15 km). A value at the upper limit of *typical* fans is qualitatively in keeping with the regional-scale drainage basin which supplied this system.

Three-dimensional evolution of the growth fold

The sequential restoration of three cross sections (Fig. 5) in up to nine steps presented in Ford *et al.* (1997) provides a model for the development through time of the Sant Llorenç de Morunys growth fold. Restoration is based on classical section balancing techniques (Dahlstrom 1969; Hossack 1979), driven principally by line length balancing, but with constant volume control. Successively older stratigraphical boundaries that approximate bedding are restored to horizontal about a hinterland pin-line. The pin-line was positioned such that negligible distortion was generated across the complex geometries of the anticlinal crests. This was dictated by the observation that in this hinge zone major and minor unconformities record no displacement or distortion. Based on these restorations we attempt here to reconstruct the three-dimensional palaeogeographical environment and lateral variations in fold growth history at Sant Llorenç de Morunys. Based on field observations (summarized above), sequential section restoration and numerical modelling it was concluded in Ford *et al.* (1997) that the Sant Llorenç de Morunys folds grew predominantly by limb rotation but that limb lengthening also occurred, induced principally by the deposition of dip-parallel wedge-shaped sedimentary bodies (formational lithosomes).

Using stratigraphical architecture (e.g. offlap–onlap–overlap), principally recorded in the crestal regions of the growth anticline, four periods of fold growth have been recognized. In this study we depend entirely on growth geometries as, currently, no control on absolute time intervals is available. Within the growth syncline we have to assume ongoing sedimentation, as periods of non-deposition or even erosion generally cannot be recognized. Stratigraphical geometries are controlled by the interaction of sedimentary processes and growth of the fold pair (Burbank & Vergés 1994; Artoni & Casero 1997). We attempt to track this relationship on a very large scale by a graph of time against the relative rates of sedimentation (R_s) and fold growth (uplift, R_u) for each of the profiles (Fig. 14a). Vertical movements due to fold growth are relative to the sedimentation base level. As the fold developed at the Earth's surface R_u is the rate of surface uplift as defined by England & Molnar (1990). Increased R_u relative to R_s can lift the crest of the anticline above base level inducing erosion. In the syncline the same change will simply reduce the amount of sedimentation. Thus the anticlinal crest is the most sensitive area of the growth fold to changes in R_s/R_u. On a short time-scale sedimentation and tectonic activity are periodic in these environments (e.g. Wolman & Miller 1960; Heward 1978; Suppe *et al.* 1997); however these fluctuations are not visible on the longer time scale implied in Fig. 14a. When the anticlinal closure is considered in more detail (see below) the episodic nature of both sedimentation and fold growth can be detected with packages of sediment separated by unconformities that are subsidiary to the principal unconformity. The gross evolution of the Sant Llorenç de Morunys growth fold which is visible and analysed in this paper involves a general decrease in fold growth with respect to sedimentation, as previously detected by Riba (1973). In other words fold activity was dying out. This process was diachronous so that folding was still active to the east while to the west the inactive part of the structure was being buried. An idealized growth fold showing four stages of fold demise (A to D) is represented in Fig. 14b. Although these four

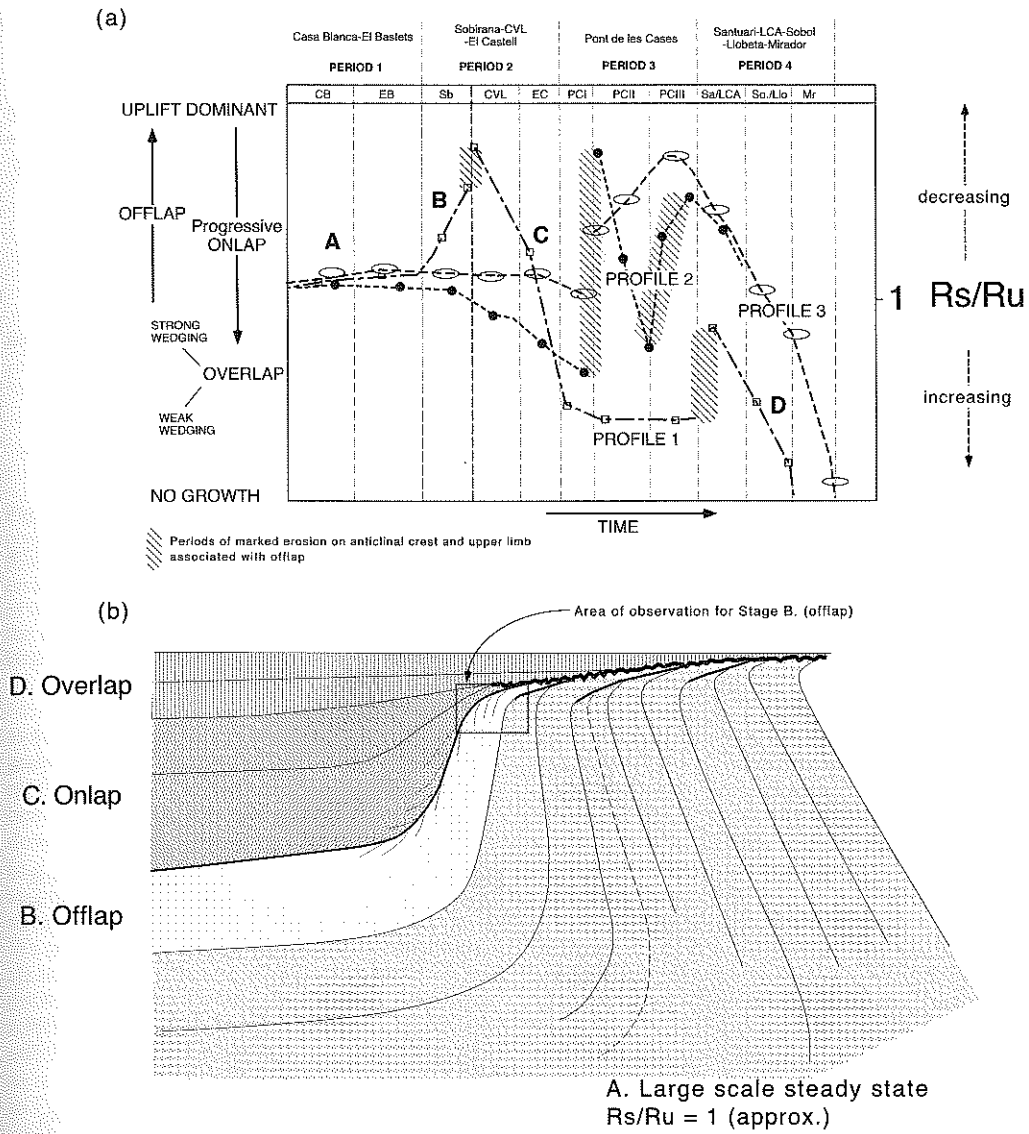

Fig. 14. (**a**) Graph showing the ratio of rate of uplift (R_u) to rate of sedimentation (R_s) for the three cross sections through the Sant Llorenç structure. (**b**) Schematic growth fold showing four stages of fold demise (A–B). These stages are seen in all three cross sections of the Sant Llorenç de Morunys growth fold but at different times due to the diachroneity of fold demise.

stages of fold demise can be recognized on each profile, they do not correspond to the four periods of evolution of the Sant Llorenç de Morunys fold pair as a whole because fold demise was diachronous along strike. In our idealized fold, the system is relatively stable during stage A with R_s and R_u approximately equal but fluctuating. The anticlinal axial plane would therefore lie either directly above or below (as in Fig. 14b) the principal unconformity. During stage B a prolonged decrease in sedimentation rate with respect to uplift rate causes a major period of growth offlap followed in stage C by an increase in R_s relative to R_u causing growth onlap. Finally in stage D, overlapping strata show gradually weaker wedging indicating a decrease in tectonic activity. Variations on this general model which represent variation in

sedimentation and tectonic processes during fold development across the region will be discussed below.

Block diagrams representing palaeogeography during periods 2 to 4 have been constructed to illustrate the three-dimensional variations in sedimentation, erosion and fold development. The diagrams are based on stages in the sequential restoration of the three cross-sections. The diagrams show the Cadí thrust sheet, comprising Eocene limestones, advancing toward the foreland and a transfer zone (Schumm 1981) between the thrust (mountain) front and the fall line. We show a hypothetically located bedrock exit canyon in the Cadí thrust sheet to emphasize that large volumes of exotic sediment were supplied to this region over the time scale of an epoch. The nature of the detritus suggests linkage to a large-scale drainage basin, and therefore probably a sub-permanent exit canyon of the type related to the half width-scale of the orogen (Hovius 1996). To the south of the fall line the depositional surface is underlain by the growing fold pair. There are several uncertainties involved in these models, in particular in the character and size of the sediment transfer area between the fall line and the tip line of the Cadí thrust sheet to the north which controlled the palaeotopographic mountain front. The width of the transfer zone must however have been sufficiently large, and persisted over the entire history of the growth structure, to have excluded any highly proximal alluvial fan facies, such as avalanche, rock slide, rock fall deposits, talus cones and colluvial slides (Blair & McPherson 1994*b*), from the depositional area. While we cannot constrain on what time scale deposition and erosion occurred across this zone, it is likely that these parameters were in long-term equilibrium, for the following reasons. (1) Incised upper fan channels supplying the Berga Conglomerates must have traversed this region and switched regularly to judge by the contrasting lithosomes and their palaeoflow (see below). If sediment did not completely by-pass this zone, aggradation would have proceeded over wide areas. (2) No petrographic signature of the Middle Eocene marine rocks, incorporated into the steep panel beneath the transfer zone, is known in the Berga Group, favouring net aggradation in this zone.

Sediment dispersal within the depositional system as recorded by palaeocurrent data for each period is integrated with the palaeogeographical models. These data provide information on the interaction between the growing fold and the depositional system.

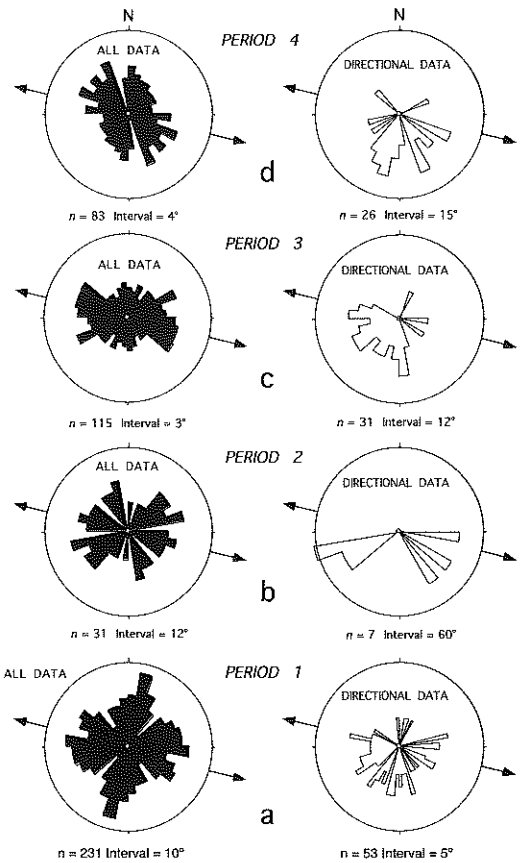

Fig. 15. Rose diagrams of combined directional and non-directional palaeocurrents for (**a**) Period 1 (Casa Blanca to Sobirana Formation times), (**b**) Period 2 (Camps de Vall-llonga–El Castell Formations), (**c**) Period 3 (Pont de les Cases Formation) and (**d**) Period 4 (Les Cases Altes–Mirador Formations). *n* refers to the number of readings, Interval is the class interval of the histogram, and the radius of the circle is 10% of points in all cases. Arrows outside the circles indicate the trend of the growth fold axes (104-284°). The vector mean for the aggregate data for Period 2 (b) is 085°, although the very low Von Mises concentration parameter k (= 0.39) indicates that this is not statistically significant.

Period 1 (Casa Blanca–El Bastets Formations)

In this paper we redefine this period to include only the Casa Blanca and El Bastets Formations (cf. Ford *et al.* 1997), because the Sobirana Formation records a clear decrease in R_s/R_u (Fig. 14a) heralding a change in growth fold dynamics. The period 1 succession forms part of the steep panel (Fig. 4) and thus reveals little about growth geometries. As the fold closures are not preserved (or exposed) there are few data

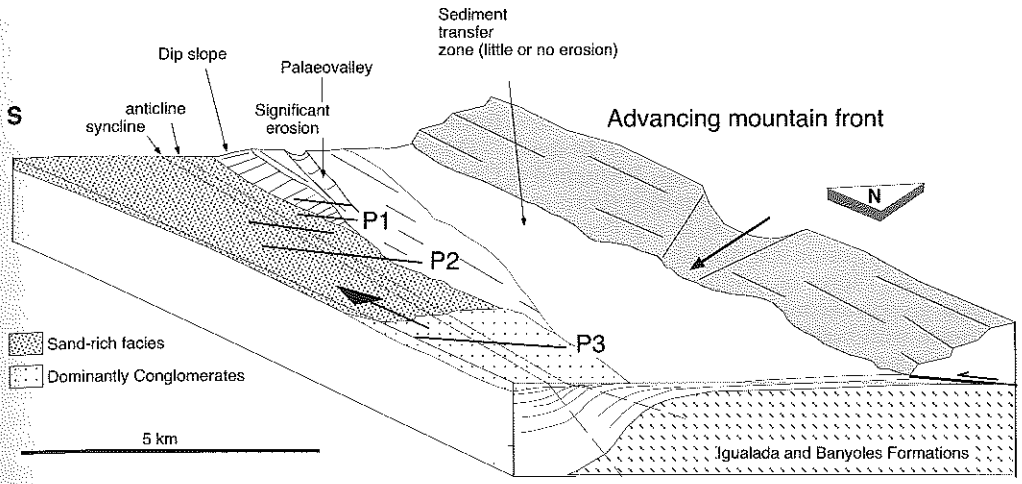

Fig. 16. Block diagram of the palaeogeography during the Camps de Vall-llonga Formation (Period 2). The position of the Cadí thrust sheet is unconstrained. In all reconstructions we show some palaeotopography on this limestone-dominated thrust sheet, including a hypothetical bedrock canyon providing a conduit for erosional material from the drainage basin to the north to the foreland basin to the south. The actual position of this conduit is unknown. This block diagram is not constrained by restored cross sections and is therefore the most schematic of those presented. The mean palaeocurrent direction is obliquely axial as shown by the large arrow. Positions of the three profiles are for reference. All reconstructions are to scale.

available to indicate the character of the fold growth before deposition of the Sobirana Formation and therefore no reconstruction has been attempted for this period. However the down-dip thickening of parts of these sequences (e.g. El Bastets Formation) are interpreted as sedimentary and indicative of growth during earlier evolution of the fold (Ford *et al.* 1997). We envisage that the growth fold developed steadily throughout this period and thus the anticlinal hinge may have described a sub-horizontal array of en echelon segments which lies above the present day erosion surface, (Fig. 14a; as in stage A of the idealized fold development in Fig. 14b).

The Casa Blanca Formation comprises a major conglomeratic lithosome in the eastern sections of the growth structure, which expanded to the WNW with time (Fig. 2). These conglomerates are laterally equivalent to a sandstone-rich unit from which the palaeoflow data was measured (see below). On a larger scale, the Casa Blanca and El Bastets Formations show a mutual thickening–thinning relationship (Fig. 4), in which the El Bastets Formation thickens to the ESE. The large-scale wedge-shaped units may represent individual fan units, bounded by surfaces which are apparently gradational and diachronous.

Sediment dispersal. Data for period 1 (Fig. 15a) indicate that two distinct directions of palaeoflow operated: (i) a transverse mode with a mean vector to the SSW and (ii) an axial mode of greater dispersion sub-parallel to the orientation of the growth fold axes. The latter mode suggests that older lithosomes responded to controls on dispersion similar to those which operated in the younger units where the growth folds are exposed. These steeply dipping strata would have been deposited to the south of the axial trace of the growth anticline. Directional palaeoflow data for period 1 (Fig. 15a) shows that the axial mode was west- and WSW-directed, though small numbers of data indicate a minor opposite flow. The transverse mode was SSW to SSE.

The bulk of the data for period 1 are restricted to the west in the Casa Blanca and El Bastets Formations. Examination of these data stratigraphically (Fig. 19) shows an upward-increasing tendency towards axially oriented flows. The upper El Bastets Formation is the first unit to show this dominance. The Casa Blanca Formation palaeoflow indicates a weak WSW–ENE mode, slightly oblique to the statistical fold axis orientation. Despite the tendency to axial flow dominance later in period 1, the palaeocurrent distributions in *c.* 50 m vertical sections suggest that individual transverse and axial mass flow and other flow type events occurred approximately in grouped packages, superimposed by fewer variant directions.

Period 2 (Sobirana–Camps de Vall-llonga–El Castell Formations)

The Sobirana Formation (Fig. 2) is an extensive sheet-like unit, approximately 100 m thick, traceable across the steep panel (Fig. 4). In the west (Vall de Lord) the Sobirana Formation shows offlap/apical wedge geometries (Ford *et al.* 1997) indicating that here R_s/R_u was decreasing (Fig. 14a). Erosion was probably ongoing to the north. As shown on profile 1 (Fig. 5a) the principal growth unconformity appears to merge southward with bedding at the top of this formation. Strata in similar positions have been eroded on profiles 2 and 3 (Fig. 5b, c).

After the deposition of the Sobirana Formation, the Camps de Vall-llonga Formation, a sand-rich sequence with limited exposure in the Cardener river bed, appears to record a significant and abrupt offlap on profile 1 followed by gradual onlap. Prolonged erosion, probably accompanying the offlap event (i.e. a period of non-deposition) and deposition of this unit, occurred to the north, further developing the principal unconformity. The 50 m deep strike-parallel palaeo-valley (Fig. 5a) seen on profile 1 was eroded around this time. The importance of this period of non-deposition and erosion further north can be appreciated when the level of the anticlinal closure on either side are compared. Above the unconformity the anticlinal closure lies at or just below river level in the Camps de Vall-llonga Formation (Fig. 5a) while the anticlinal closure for the older Sobirana Formation must have lain above the present position of the principal unconformity. On profile 2 anticlinal closures are preserved just below the principal unconformity in the Camps de Vall-llonga Formation, indicating that the growing fold pair evolved steadily with the level of erosion just above the level of the anticlinal closure (Fig. 5b) and the fall line tracked southward some distance north of the migrating anticlinal hinge. This implies that R_s was close to R_u (Fig. 14a, b). The anticlinal closure for this stratigraphical level has been eroded from profile 3 (Fig. 5c), however the Camps de Vall-llonga Formation is dominated by conglomerates in the east (Tresserres region, Fig. 4). Figure 16 schematically represents the palaeogeography for the Camps de Vall-llonga Formation showing the predominance of erosional features, offlap and sand-rich facies in the west, slight overlap in sand-rich facies in the centre and the incoming of conglomeratic facies in the east. The distribution of these features indicate that R_s/R_u increased eastward, either due to increasing sediment supply or decreasing tectonic activity. The facies change from west to east suggests that the western part of the basin may have been starved of sediment at this time while the main influx of conglomerates was further east.

On profile 1 onlapping geometries in the El Castell Formation record an increasing R_s/R_u (Figs 14a, 17 & 18). The formation eventually overlapped the principal unconformity and filled the palaeovalley along with a 25–30 m thick breccio-conglomerate unit while the growth fold pair to the south controlled wedging geometries. The El Castell Formation on profile 2 abruptly overlapped the anticlinal closure and was deposited horizontally across the upper limb (Fig. 17). This formation shows considerable thickening and numerous internal unconformities across the anticlinal closure (Figs 17 & 18c) suggesting that the anticlinal hinge zone was the focus of periodic, local erosional events. The El Castell conglomerates die out to the east (Fig. 4) and are replaced by sand-rich facies. Figure 18b schematically represents the palaeogeography at the end of El Castell times showing that, by a steady increase in R_s in the west and centre, topographies created during the earlier sediment-starved phase were infilled and overlapped to produce a smoothed depositional surface. Note that the polarity of the conglomerate to sand-rich facies change has changed in this formation indicating that the main input point for the El Castell Conglomerate lay around profile 1 or further west.

Sediment dispersal. Sediment dispersal during period 2 (Fig. 15b) was both sub-parallel to the growth structure and obliquely transverse to it. Palaeoflow data for the early part of period 2 is derived from the sandstone-rich lithosome of the Camps de Vall-llonga Formation, on the steep fold limb (i.e. originally south of the growth anticline) located in the central to eastern-central part of the structure (Fig. 19). Flow was obliquely axially-directed (Fig. 19), with the principal component to the WSW and a minor component to the ESE, although this is based on limited data. This apparent switch of flow direction may in this case be a function of flow into an interfan (sand-rich) low. The presence of a *c.* 50 m-deep valley on the principal growth unconformity incised into steep beds of the El Bastets Formation on the western side of the Vall de Lord (Fig. 5a) is evidence of a sub-axial supply of sediment during Camps de Vall-llonga time. The palaeovalley is exposed in an approximately transverse section, and suggests that in degradational regions north of the growth anticline flow was sub-parallel to the

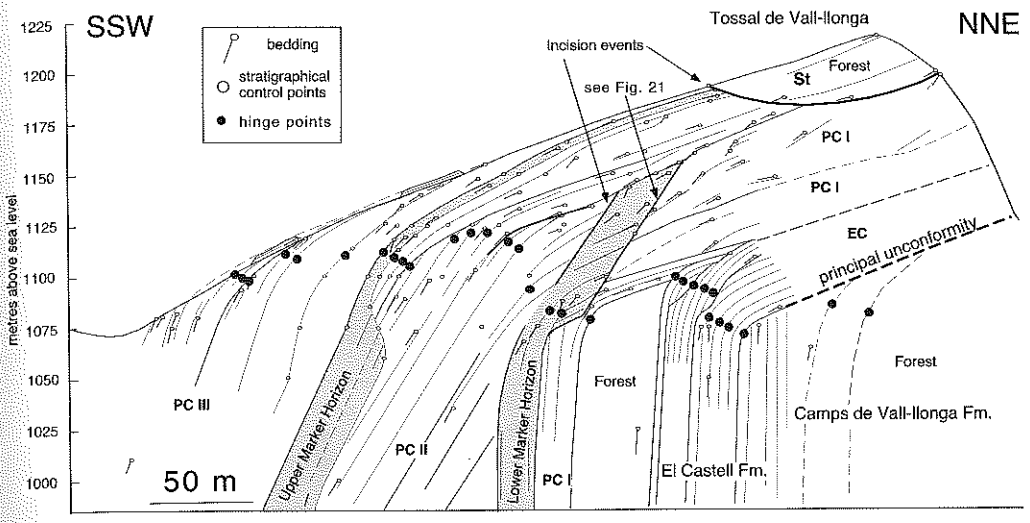

Fig. 17. Detailed cross-section of the growth anticline hinge region on the eastern side of Tossal de Vall-llonga. This shows the stratigraphical-structural relationships generated across the anticline principally during Pont de les Cases Formation times (Period 3 – post-El Castell Formation). Note the interaction of incision and sedimentation events with deformation of the topographic surface controlled by the location of the axial surface trace of the growth anticline. The principal unconformity terminates basinward within the El Castell Formation.

structural grain. During late period 2, palaeoflow in the western El Castell conglomeratic lithosome was across the trend of the growth structure, but not strictly transverse (Fig. 19). These measurements were taken in the back limb of the growth anticline, i.e. in sediments deposited to the north of the growth fold pair. Distinctly axial modes are not developed, instead a mode with a vector mean to the SW is prominent. Stronger transverse flow many have been facilitated by the burial of earlier palaeotopography by the overlapping El Castell Formation.

Period 3 (Pont de les Cases Formation)

The growth fold geometries of the Pont de les Cases Formation are the best preserved of the study area and hence a more detailed description of fold development can be presented for this period. These strata record clear variations in growth geometries and facies across the region (Fig. 5) and represent the most tectonically active period in the centre and east of the structure.

In the west (profile 1), the growth fold pair was overlapped and all units show weak wedging across the fold hinges during period 3 indicating relatively high (and increasing?) R_s/R_u (Figs 14a & 20a). Units appear to have been deposited horizontally and with constant thickness across the upper limb of the growth anticline indicating little rotation of this limb.

Further east (profile 2), accelerated fold growth provided more accommodation space in which a thicker Pont de les Cases Formation accumulated. Probably one of the best exposed growth anticlines in the world is found on Tossal de Vall-llonga (Fig. 4; profile 2, Fig. 5b), the details of which are presented in Fig. 17. Here the lowest member, PC I, overlapped across the upper limb of the anticline but was subsequently largely incised and eroded from the anticlinal crest (Figs 17 & 21). When restored, the strike-parallel incision has a maximum dip of 35° south, a minimum height of 40 m but does not extend beyond 200 m to the west. A 50 cm thick, reddened, matrix-supported breccia lies along the erosion surface. This palaeoriver margin was probably formed by flow parallel to the anticlinal crest by a channel localized on the hinge. The southern margin of the channel appears to lie some 150 m down dip in a poorly exposed area of the steep limb where the boundary of the lower marker horizon steps southward. This large channel relief was infilled and buried by the lower marker horizon, a limestone rich breccio-conglomerate (Fig. 21) which extends beyond the channel margins. The areal distribution of this unit suggests that it was deposited as a small fan lobe-like body (Fig. 22), which locally infilled this channel feature, reaching a

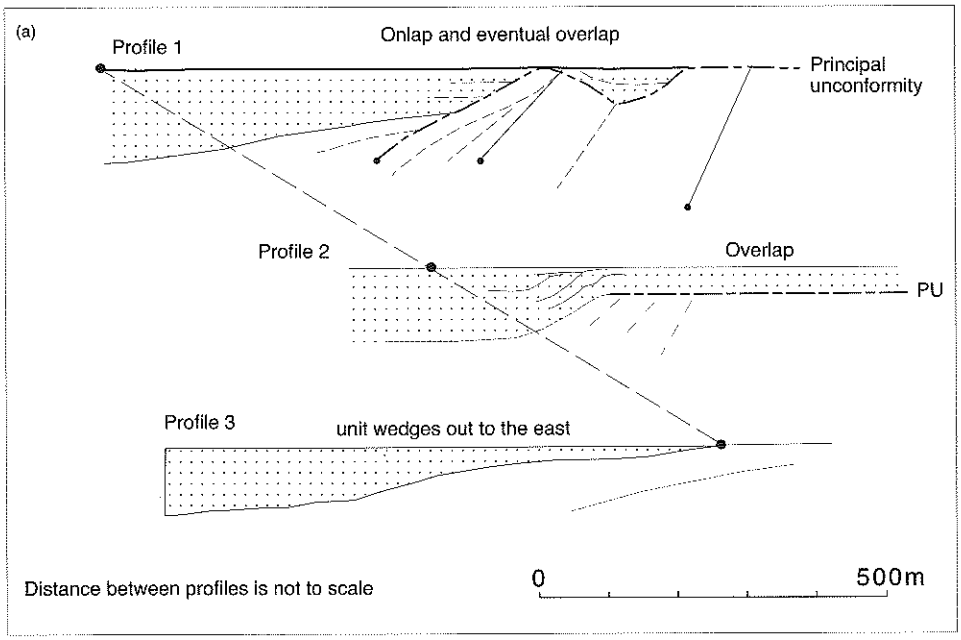

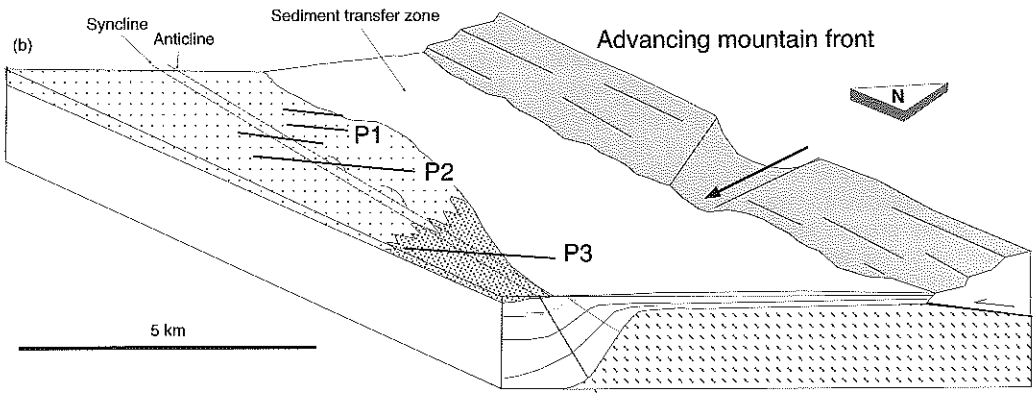

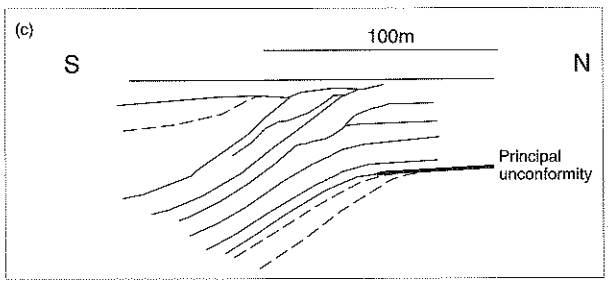

Fig. 18. (**a**) Restored geometry of the El Castell Formation from profiles 1, 2, and 3, linked by pin line. (**b**) Block diagram of the palaeogeography during the El Castell Formation (Period 2) showing on profile 1 onlap of previously formed topography and eventual overlap to fill the palaeovalley to the north. On profile 2 the formation overlapped the anticline continuously. The unit wedges out to the east. See Fig. 16 for key to patterns. (**c**) Detail of restored geometry of the El Castell Formation on the hinge of the anticline on profile 2.

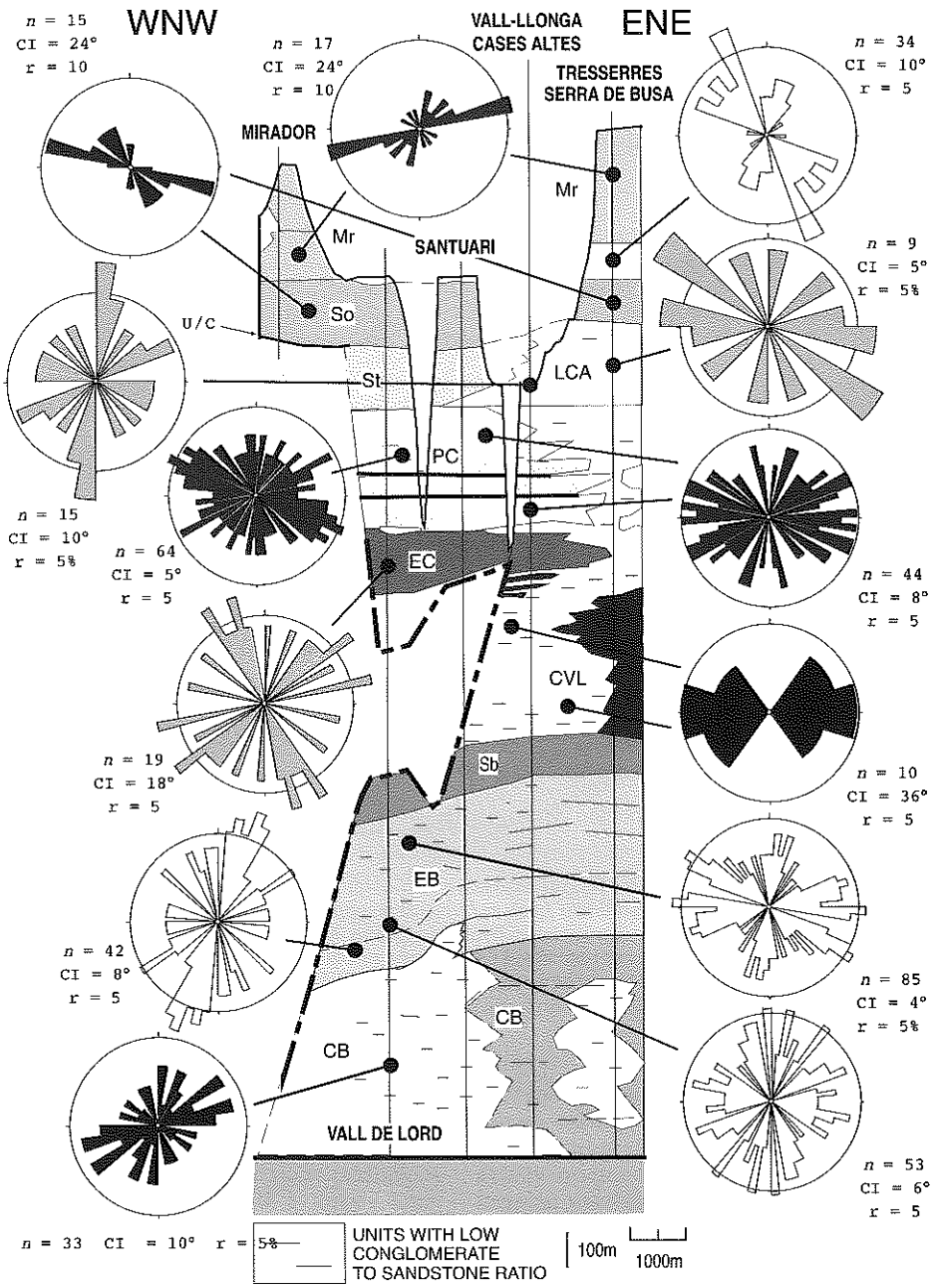

Fig. 19. Palaeoflow data subdivided stratigraphically and spatially through the growth structure. All rose diagrams display palaeocurrents in a non-directional form; north in all cases is to the top of the page. *n* refers to the number of data, CI is the class interval of rose diagram. The radius (*r*) of the scale circles is either 5% of points or the specified value of r times the normal distribution. Refer to Figs 2 and 3 for more details of the Berga Conglomerate Group lithostratigraphy.

thickness of 40 m. Elsewhere the unit is only 5–10 m thick. Palaeoflow in the upper beds of the lower marker horizon adjacent to the palaeo-river margin show transverse flow. The lower beds of member PC II record a later period of incision and infill localized on the

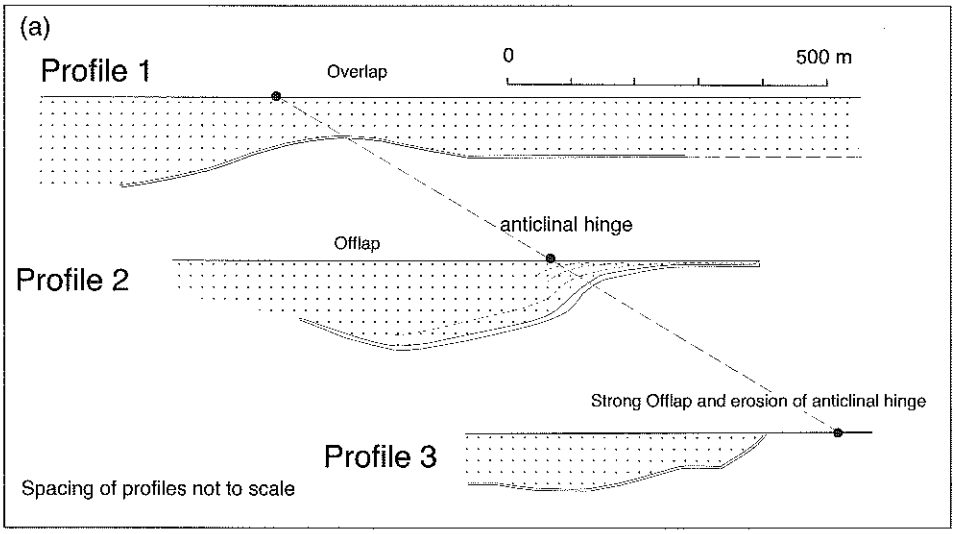
(a)
Profile 1
Overlap
0
500 m
anticlinal hinge
Offlap
Profile 2
Strong Offlap and erosion of anticlinal hinge
Profile 3
Spacing of profiles not to scale

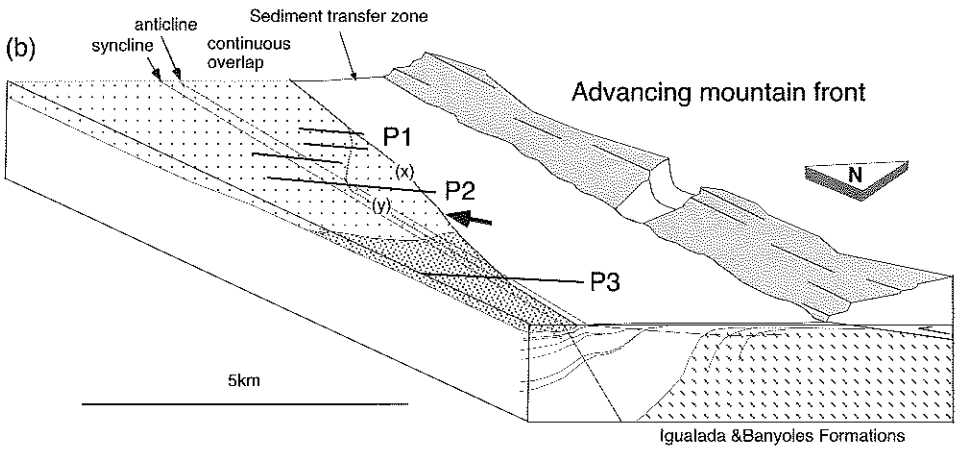
(b)
anticline
syncline
Sediment transfer zone
continuous
overlap
Advancing mountain front
P1
(x)
P2
(y)
P3
N
5km
Igualada &Banyoles Formations

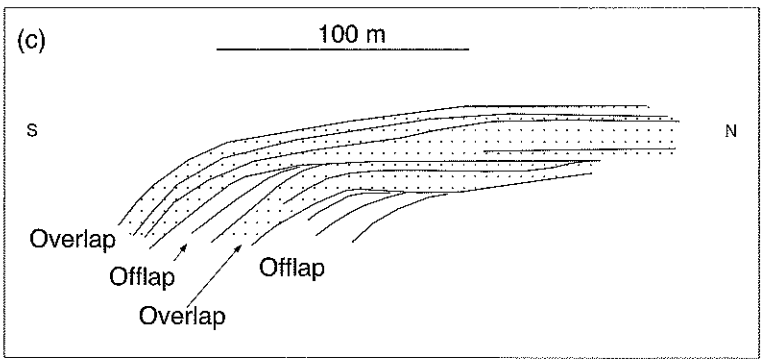
(c)
100 m
S
N
Overlap
Offlap
Offlap
Overlap

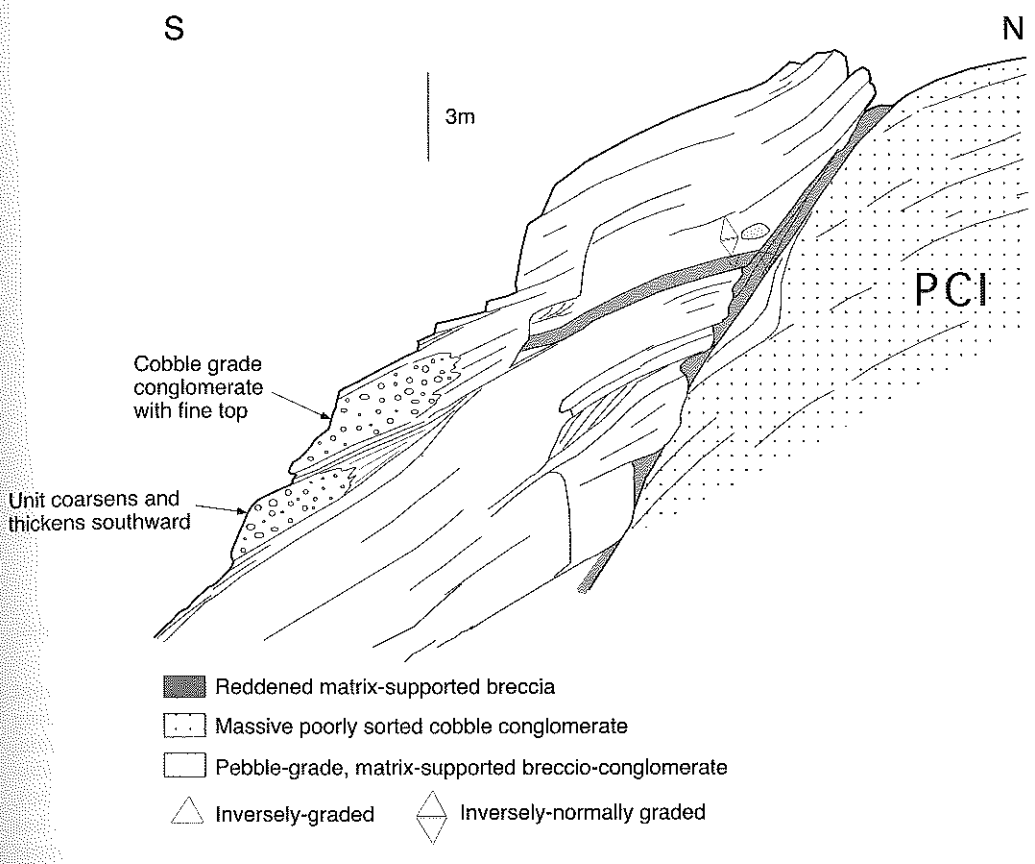

Fig. 21. Field sketch of northern margin of an incised palaeochannel (see Fig. 17) exposed on the eastern side of Tossal de Vall-llonga. This exposure is approximately 5 m deep, climbing away from the viewer. The palaeocliff surface, defined by a 0.5 m thick unit of reddened matrix-supported breccia is continuous but hidden in places by projecting rock units in this view. To the north conglomerates belong to member I of the Pont de les Cases Formation (PCI). The lower units of the Lower Marker Horizon infill the palaeotopography. The depositional dip of the fill abutting the margin is very low, and does not represent angle of repose stratification of a talus cone or scree.

growth anticline hinge (Fig. 17) that cut into the lower marker horizon. The upper units of PCII very clearly record alternating phases of offlap and overlap (Fig. 20c). These short periodicity events were superimposed on a longer time-scale increase in R_s/R_u in the middle levels of this formation (Fig. 14a). Continuous growth offlap dominated in the upper member PC III (R_s/R_u decreased; Figs 14a & 20). A 25 m deep incision on the peak of Tossal de Vall-llonga (Fig. 17) may have occurred synchronously or following this period of growth offlap. The (concave) form of the erosion surface implies the base of a sub-axially oriented valley, possibly favoured by location over the northern limb of the growth anticline, where subsidence was more likely to be attenuated, and entrenchment promoted.

To the east (profile 3, Fig. 5c) the Pont de les Cases Formation is significantly thinner in the core of the syncline than on profile 2 and

Fig. 20. (**a**) Restored geometries of the upper member of the Pont de les Cases Formation (PCIII) on the profiles 1, 2 and 3, linked by a pin-line. (**b**) Palaeogeographical block diagram of the growth structure at the end of Period 3 (Pont de les Cases Formation). The heavy arrow indicates the approximate entrance point of a probable incised fan channel. As shown in (a) the formation changes from overlap geometries in the west to strong offlap and erosion in the east. On profile 2 the geometries varied from overlap (x position of fall line) to offlap (y position of fall line) through time. (**c**) Detail of growth geometries within the middle member of the Pont de les Cases Formation (PCII) on profile 2, showing alternating offlap and overlap.

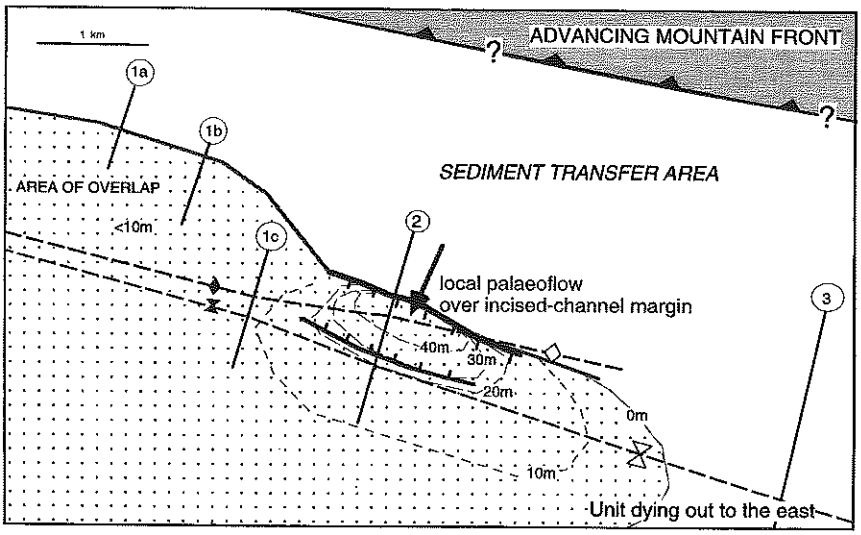

Fig. 22. Palaeogeographical map of the Lower Marker Horizon (within the Pont de les Cases Formation) showing infill by this unit of an erosional-topographical feature on Tossal de Vall-llonga (see Figs 17 and 21).The position of the advancing Cadí thrust sheet is unconstrained. Palaeoflow outside this feature was axial.

sand-rich facies are dominant (Figs 2 & 20). The main input point for conglomerates at this time lay therefore to the west. The lower member PC I thins gradually upward along the steep limb (Fig. 5c) and may have overlapped the anticline as in profile 2. The upper two members appear to offlap but their history is difficult to establish with certainty because of the presence of an unusual local unconformity at the base of the overlying Les Cases Altes Formation. In the steep limb this surface is bedding parallel, separating PC I and Les Cases Altes Formation. However toward the hinge of the syncline the surface cuts across the PC II and PC III members. The details of this structure is shown in Fig. 23. The boundary is complicated by a lateral (N-S) facies change in the upper part of PC III (sand to the south). Because it truncates PC II and III this unconformity may record a phase of erosion post-dating deposition of PC III. However several observations suggest a more subtle structure. At several points just below the unconformity, dips in the underlying conglomerates appear to fan rapidly from steep values upward to parallelism with overlying beds suggesting evolution as a progressive unconformity associated with growth offlap. However the surface becomes bedding parallel to the north and to the south and can only can be traced laterally for over 1 km. This feature is important (1) because it demonstrates that significant erosion (whether progressive or abrupt) can occur close to or even in the core of the growth syncline and (2) because it has important implications for the nature of the folding mechanism. The trace of the growth syncline, continuous on profiles 1 and 2, is clearly displaced across this unconformity (Fig. 5c). Numerical modelling (Ford *et al.* 1997) has shown that this cannot be reproduced by simple models of kink band migration but can be reproduced by a limb rotation (trishear) model by incorporating a significant break in sedimentation.

Figure 20b shows a block model for the area at the end the Pont de les Cases Formation. Conglomerates were fed into the western part of the structure, while a sandstone-rich lithosome was deposited in the east. R_s/R_u is thus interpreted to have decreased to the east (Fig. 14a). In addition, the fold clearly amplified to the east at this time, contributing further to an eastward decrease in R_s/R_u. This is reflected in the continuous overlap on profile 1 (Fig. 20a), changing to the more complex history on profile 2 (Fig. 20c) which itself records a decrease in R_s/R_u with time through the formation. The, as yet unresolved, structures of profile 3 which record a complex interrelationship between offlap, erosion and a break in sedimentation, all indicate a decreasing R_s/R_u with time, but perhaps not as gradual as in the region of profile 2.

Sediment dispersal. Aggregate data for period 3 indicates that axial-parallel palaeoflow dominated over transverse dispersal (Fig. 15c). This

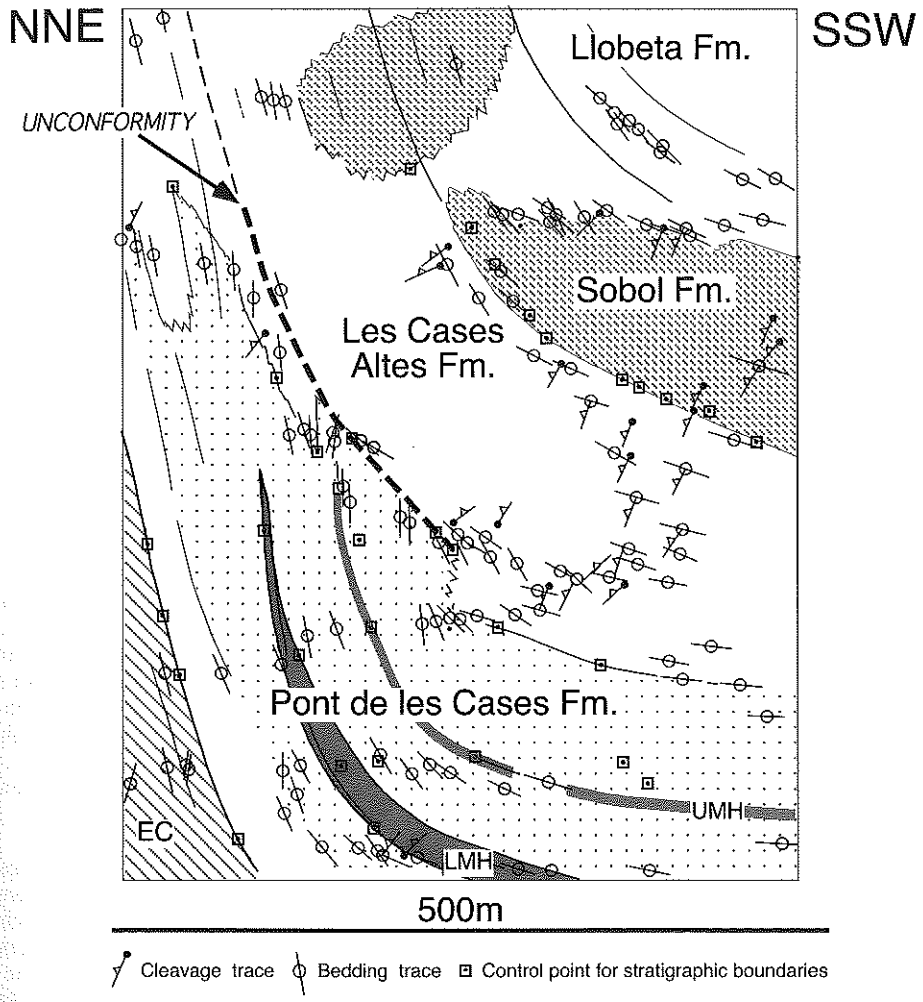

Fig. 23. Detailed cross-section through zone of composite off-onlap ('progressive unconformity') on profile 3. (see Fig. 5c for location) showing progressive changes in dip through several levels across the unconformity, and the geometries of the associated lithosomes. White units are sand-rich.

period shows the most strongly developed axial flow in the history of the structure, and appears to have been closely related to the axial trace of the growth folds. Data collected from the complex, dominantly conglomeratic lithosomes in the west and centre of the structure, show west- and WNW-directed flow (Fig. 19). The directional dataset (Fig. 15c) also indicates south-directed palaeoflow modes. The gradual ESE termination of these lithosomes, and replacement by finer-grained, sandy equivalents suggest that a major transverse/high-angle entry point, which supplied dominantly gravel, was located between profiles 2 and 3, as indicated by the arrow in Fig. 20b. This may have been controlled by the relative uplift (lower rates of subsidence) of the structure in the east, as indicated by the offlapping stratigraphy during this period.

The predominant axial palaeoflow is also reflected in the series of large-scale erosional structures revealed in the central regions of the growth structure (Fig. 17). The axial surface trace of the growth anticline is associated with major incision surfaces immediately pre-dating (Fig. 21) and post-dating the lower marker horizon, the latter an *apparently* 'one-sided' incision, possibly representing a palaeocliff (Fig. 17). The planar, strike-parallel form of this, and the steeply-incised channels, suggests alluvial

down-cutting by water flows parallel to the anticline trace. However, although hanging valleys (or canyons) are not observed incised into period 2 gravelly alluvium in the region of profile 2, the fan-lobate form of the lower marker horizon (Fig. 22) suggests an apical entry point at (and crossing) the northern margin of the palaeochannel. This implies a transverse drainage across the surface trace of the anticline which acted episodically as a local fall line during period 3, e.g. during lower marker horizon aggradation. The characteristics of this and the upper marker horizon (restricted sedimentary clast assemblages, higher angularity and immature shapes) suggest either (1) a short transport path from a relatively small drainage basin in the frontal ranges of the mountain front or, perhaps less likely, (2) reworking of local material from the erosional/non-depositional region to the north of the growth anticline (Fig. 22). The less well defined limits of the overlapping upper marker horizon, though similar to those of the lower marker horizon in the east, suggests a similar interval of transverse drainage across the anticlinal crest, possibly preceded by axial erosional flows (Fig. 17). No palaeocurrent data yet exists for the Pont de les Cases Formation on the back limb of the growth anticline to compare the dispersal with that in the common limb and syncline. The dominantly conglomeratic members PCI to III showing W and WNW palaeodispersal thus alternated with probably shorter intervals of localized transverse dispersal represented by the marker horizons.

Period 4 (Santuari–Les Cases Altes–Mirador Formations)

Above the Pont de les Cases Formation the entire growth structure is dominated by growth overlap (Fig. 5), which followed a phase of early onlap in the east, as folding died out and the structure became buried. Thus sedimentation rates everywhere became greater relative to fold growth rate (Fig. 14a; equivalent to phase D in Fig.14b). In the west (profile 1), the upper limb of the growth anticline was tilted and eroded (R_s/R_u decreased) during deposition of the Santuari Formation, which tapers strongly across the fold pair. The resultant erosion surface steps up proximally across a 100 m high strike-parallel cliff (Fig. 24a, b; see also Ford *et al.* 1997, fig. 7). The Santuari Formation forms a rapidly eastward-tapering conglomeratic lithosome, interfingering with the laterally equivalent sand-rich Les Cases Altes Formation (Fig. 24b). The overlying Sobol and Mirador Formations overlapped the entire western area and record an upward decrease in growth. The Sobol Formation banked against the cliff, which was itself probably only a few hundred metres south of the mountain front.

On profile 2 the Santuari Formation overlapped the growth anticline and infilled a 50 m incision into older beds of the upper limb on Tossal de Vall-llonga (Fig. 17). The geometries of younger units across the growth anticline are not preserved, however the syncline is clearly developed in the Sobol Formation (Fig. 5b). On profile 3 the lower beds of the Les Cases Altes Formation show growth onlap (Fig. 5c) across the top of the Pont de les Cases Formation in the hinge of the growth syncline, while upper beds formed an apical wedge. The growth anticline is preserved in overlying formations (Fig. 5c) which show growth overlap continuing into the uppermost levels of the Mirador Formation (Fig. 24c). These relationships suggest that in this eastern area sedimentation rates were high and that fold growth continued while further west folding died out and local development of accommodation space was reduced.

Sediment dispersal. Data for period 4 (Figs 15d & 19) indicate dominant oblique-transverse palaeoflow to the SSW. The sandstone-rich Les Cases Altes Formation had differing dispersal in the west (dominantly transverse) to in the east (oblique-axial; Fig. 19). The similarly sandy Llobeta Formation, restricted to the eastern parts, dispersed sediment to the SSE (Fig. 19), the data extending to the south limb of the Busa syncline (Fig. 4). Only the Sobol conglomeratic sheet-like lithosome dispersed sediment in an approximately axial parallel direction during period 4 , possibly influenced by the cliff feature in the NW of the structure and a WNW–ESE fall line in the east (Fig. 24b). Palaeodispersal within the overlapping Mirador Formation, although based on few data, shows (i) an oblique transverse SW mode in both the west and east of the structure, and (ii) modes directed toward the south quadrant.

Fig. 24. (**a**) Restored geometry of Sobol Formation in each of the three profiles linked by a pinline. (**b**) Palinspastic block diagram detailing the palaeogeography during Sobol Formation time (Period 4) showing the cliff in the west. Note that the folds are dying out to the west. (**c**) Palinspastic block diagram of palaeogeography during Mirador Formation time showing the continued fold activity in the east while the Vallfogona thrust is emergent in the west. See Fig. 18 for key to patterns.

(a) Restored geometries of Sobol Formation

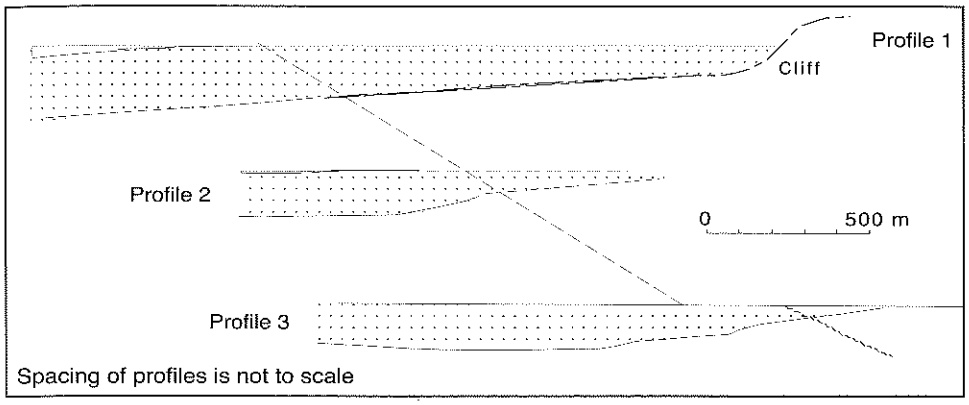

(b) Sobol Formation reconstruction

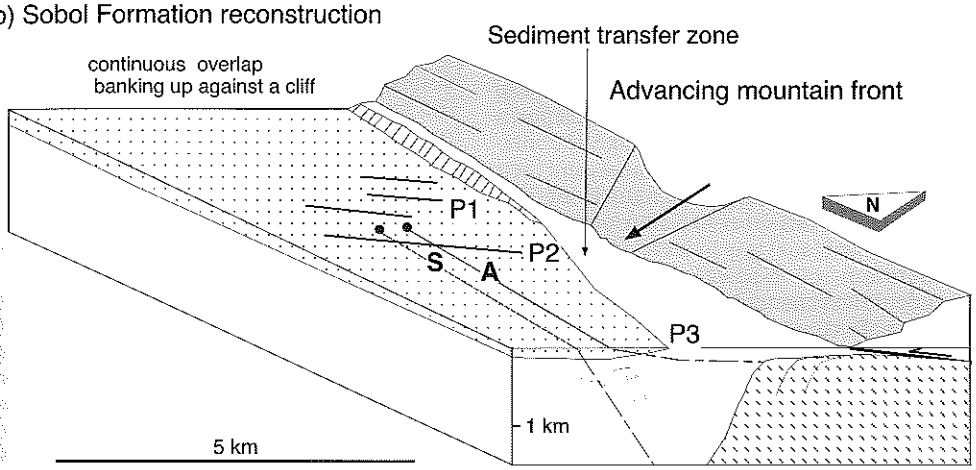

(c) Mirador Formation reconstruction

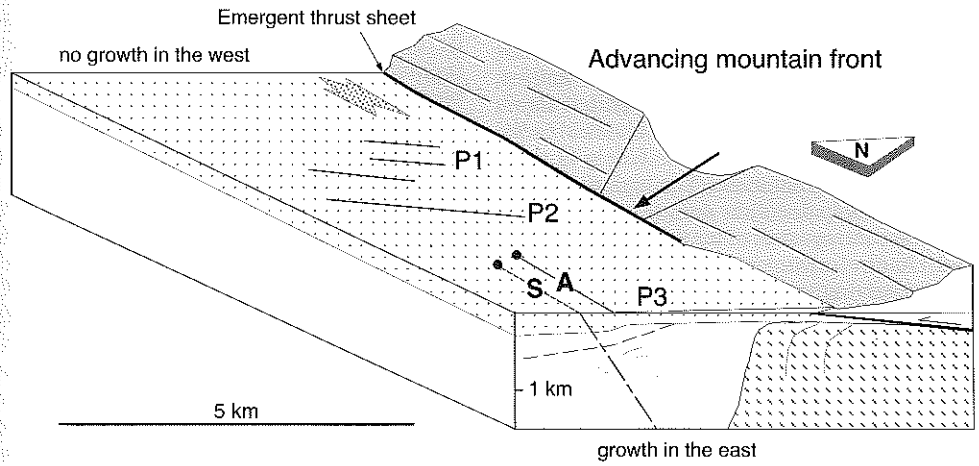

While distribution of sand-rich facies was restricted to the east during periods 3 and 4, during early period 1 and period 2 sand-rich facies were aggraded to the west of their conglomeratic equivalents. This variation is thought to be related to switching of proximal fanhead trenches (incised fan channels; cf. Denny 1967) between stable mountain front exit points and the fall line controlled by the growth structure. The contrasting along-strike evolution of the growth structure may also have had an important influence on facies distribution. In summary, growth folding died out diachronously across the area, continuing in the east after it had ceased in the west.

Discussion and conclusions

The sediments

The alluvial stratigraphical pile preserved in the Sant Llorenç de Morunys growth structure can be considered as multiple discrete event deposits covering very extensive areas, unlike the alluvium of established perennial channels and their enclosing floodplains. The nature of the emplacement of this sheet-like alluvium (related to steep alluvial fans) precludes to a large extent consideration of factors relevant to how antecedent river channels are affected by growth structures (Burbank *et al.* 1996), and also subsidence, interconnectedness and deposit density relationships of alluvial architecture models (Bridge & Leeder 1979). However, palaeodispersal patterns through the history of this structure suggest that the prevailing high concentration–high magnitude cohesionless debris flows and fluidal sediment flows were deflected by surface topography associated with, in particular, the common limb to growth syncline, and also the growth anticline. However, for sequences of tens to hundreds of metres, transverse as well as axial flows operated across the actively deforming surface. A classical radial palaeoflow pattern is not immediately obvious from the existing database. The high dispersion of much of the palaeoflow data (Figs 15 & 19) is likely to be the product of fan form and scale, fan head channel switching, fan lobe expansion angle, evolving surface slope (controlled by growth deformation) and vertical grouping of the data (up section changes with time). The mixture of structural types synthesized in the rose diagrams is thought to be less significant than the primary factors.

The bulk of the sediment volume was supplied externally to the region, and although significantly diverted at certain times (e.g. Period 3), appears to have been ultimately transferred through the growth structure to areas to the south. The length of axial (mountain front-parallel) diversion of incoming sediment is presently unknown (see below).

The effect of the growth fold on sedimentation

In comparison to most growth folds affecting foreland basin deposits the Sant Llorenç de Morunys fold pair has a quite different geometry and thus had a very different effect on the accumulating sediments. Its highly asymmetrical geometry and essentially flat-lying anticlinal back limb, which seems not to have significantly rotated throughout fold development, (1) facilitated largely unhindered sediment transfer from the mountain front and (2) resulted in growth strata being developed almost exclusively on the basinward side of the anticlinal axial surface. The back limb of the structure was cut by the frontal (Vallfogona) thrust which controlled the mountain front. Units overlapping the back limb of the anticline are horizontally-bedded, of constant thickness and extend far to the north of the anticlinal crest (e.g. the El Castell Formation on profile 2, the Pont de les Cases Formation on profile 1). Thus no simple anticinal uplift capable of acting as a barrier (e.g. Burbank *et al.* 1996) was generated by folding; subsiding areas, until late in the history of the structure, were therefore demarcated principally by the rotating and lengthening common limb. This implies that the axial surface trace of the growth syncline was the favoured site for axial diversions of palaeocurrents.

An 'intrabasinal' fall-line at the axial surface trace of the growth anticline is thought to have developed due to the change in subsidence regime from the static to uplifting anticlinal backlimb to the subsiding common limb and growth syncline. A clearer intrabasinal fall-line existed at the time of the principal unconformity. Sedimentation rates appear to have been sufficiently high throughout most of the fold history to have suppressed *major relief* potentially generated across the growth fold pair, and at the fall line generated by the principal unconformity. However, sufficient surficial subsidence occurred to have influenced palaeoflow, particularly in the earlier history of the structure (periods 1–3).

Regional context

The southern margin of the south Pyrenean thrust sheets is a complex segmentation of

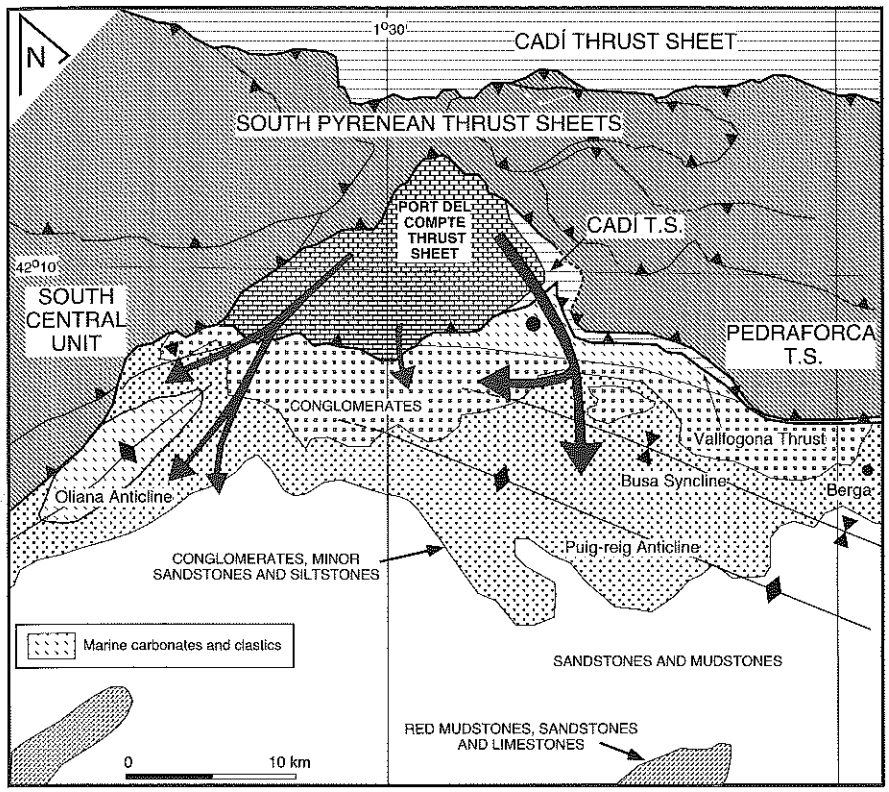

Fig. 25. Tectonic map of the SE Pyrenean Mesozoic-Cenozoic thrust sheets, and the present distribution of Late Eocene-Oligocene continental clastic facies (as in Fig. 1b), superimposed by the currently known major dispersal pathways. The longitudinal system in the Oliana area is after Burbank & Vergés (1994), and the bimodal south- and west-directed dispersal is simplified from this study. Note that both systems emerge from the re-entrant in the lower Pedraforca thrust sheet, the area presently occupied by the Port del Compte thrust sheet.

frontal and oblique ramps comprising the external thrust of the system (Fig. 25). Synchronous with the motion of the frontal thrust, the Puig-reig and Oliana anticlines developed within the foreland basin, sub-parallel to their respective thrust fronts (Fig. 25). The Oliana structure grew over a period of several million years as documented by associated growth strata (Burbank *et al.* 1992*a*; Vergés 1993).

The evolving landscape during late Eocene and Oligocene thrusting was dominated by drainage basins eroding marginal thrust sheets and the high axial Pyrenean zone, supplying sediment to the centre of the Ebro Basin. This central region was characterized by prograding subaerial terminal fans and playa lakes, for example on the northern limb of the Súria anticline, 75 km south of Sant Llorenç de Morunys (Sáez 1987; Fig. 1). Dispersal through the Sant Llorenç growth structure had distinct southward and westward modes (Fig. 25), whereas a large-scale longitudinal fluvial dispersal system was oriented parallel to the growing Oliana Anticline (Burbank & Vergés 1994), parallel to the local mountain front. Taken together these systems apparently diverge from the re-entrant displayed by the lower Pedraforca thrust, at present occupied by the Port del Compte thrust sheet (Fig. 25). This thrust sheet was emplaced at a late stage of Pyrenean shortening (Vergés 1993). The region defined by the lower Pedraforca re-entrant is interpreted as a relatively low topographic region prior to emplacement of the Port del Compte thrust sheet (Vergés 1993), at the same time as conglomerate deposition in the Oliana and Sant Llorenç de Morunys areas. It may therefore have represented a primary mountain front re-entrant or embayment. Late-stage dispersal in alluvial fan settings west of Sant Llorenç, thought to be sourced by the Port del Compte thrust sheet, is also southward-directed.

Sedimentation rates and growth strata evolution

Geomorphic evolution of the drainage basin (e.g. Schumm 1981) forced by the main phase of Pyrenean shortening, basin-scale flexural subsidence generated by thrust sheet loading (Doglioni & Prosser 1997), and potential climatic cyclicity suggest that sedimentation is unlikely to have maintained a steady long term rate. This is confirmed by several studies of successions of similar age in the Spanish Pyrenees. For example, accumulation rates varied from 0.15 to 0.5 mm a^{-1} for uppermost Eocene to upper Oligocene fluvial and lacustrine deposits of the southeastern South Central Unit at Artesa del Segre (Meigs *et al.* 1996; Fig. 1a), and conglomeratic growth strata associated with the Oliana growth anticline (Fig. 25) had rates of sediment accumulation from 0.14 to 0.25mm a^{-1}, with a low rate period of 0.06 mm a^{-1} (Burbank & Vergés 1994; Vergés *et al.* 1996). As there is no current absolute time frame for the Sant Llorenç sediments, we estimate that the minimum thickness of 2.5 km of Berga Conglomerates at Sant Llorenç were deposited in >10 Ma, extrapolating the mean accumulation rate of 0.25 mm a^{-1} calculated for the stratigraphically equivalent conglomerates at Oliana (Fig. 25; Burbank & Vergés 1994). The establishment of a reliable chronometric framework for these sediments is clearly required to specify controlling parameters by quantifying R_s and R_u. Superimposed on the above suite of controls are local processes such as the temporally and spatially variable rate of fold uplift (and subsidence), and the rate of advance and erosion of the palaeomountain front. Despite the likelihood of non-steady accumulation rates on a megasequence scale, the patterns of stratigraphical architecture and aspects of conglomerate sedimentology described in this paper suggest that variations in structurally controlled uplift and subsidence generated by the mountain front tectonic regime was a most significant variable that influenced the growth strata at Sant Llorenç for much of its history.

This work is part of a multidisciplinary study into growth fold evolution in foreland basins, as part of the EU JOULE II Geosciences project 'Integrated Basin Studies', directly funded by the Swiss Bundesamt für Bildung und Wissenschaft (project 94.0153). J.V. has been partially supported by DGICYT project PB94-0908 and by the Comissionat per Universitats i Recerca de la Generalitat de Catalunya, Quality Group GRQ94-1048. Aspects of this study were presented at the BSRG annual meeting in Dublin 1996 and at EUG 9 at Strasbourg 1997. Many thanks are due to P. D. W. Haughton and D. W. Burbank for their constructive, thought-provoking reviews, and to A. Mascle for his editorial assistance.

References

ALLEN, P. A. 1981. Sediments and processes on a small stream-flow dominated, Devonian alluvial fan, Shetland Islands. *Sedimentary Geology,* **29,** 31–66.

ANADÓN, P., CABRERA, L., COLOMBO, F., MARZO, M. & RIBA, O. 1986. Syntectonic intraformational unconformities in alluvial fan deposits, eastern Ebro Basin margins (NE Spain). *In*: ALLEN, P.A. & HOMEWOOD, P. (eds) *Foreland Basins*. International Association of Sedimentologists, Special Publications, **8,** 259–271.

ARTONI, A. & CASERO, P. 1997. Sequential balancing of growth structures, the late Tertiary example from the central Apennine. *Bulletin de la Société Géologique de France,* **168,** 35–49.

BLAIR, T. C. & BILODEAU, W. L. 1988. Development of tectonic cyclothems in rift, pull-apart, and foreland basins: sedimentary response to episodic tectonism. *Geology,* **16,** 517–520.

—— & MCPHERSON, J. G. 1994*a*. Alluvial fans and their natural distinction from rivers based on morphology, hydraulic processes, sedimentary processes, and facies assemblages. *Journal of Sedimentary Research,* **A64,** 450–489.

—— & —— 1994*b*. Alluvial Fan Processes and Forms. *In*: ABRAHAMS, A. D. & PARSONS, A. J. (eds) *Geomorphology of Desert Environments.* Chapman & Hall, London, 354–402.

BLUCK, B. J. 1967. Deposition of some Upper Old Red Sandstone conglomerates in the Clyde area: A study in the significance of bedding. *Scottish Journal of Geology,* **3,** 139–167.

—— 1976. Sedimentation in some Scottish rivers of low sinuosity. *Transactions of the Royal Society of Edinburgh: Earth Sciences*, **69,** 425–456.

—— 1979. Structure of coarse grained braided stream alluvium. *Transactions of the Royal Society of Edinburgh: Earth Sciences,* **70,** 181–221.

BRAYSHAW, A. C. 1984. Characteristics and origin of cluster bedforms in coarse-grained alluvial channels. *In*: KOSTER, E. H. & STEEL, R. J. (eds) *Sedimentology of Gravels and Conglomerates.* Canadian Society of Petroleum Geologists, Memoirs, **10,** 77–85.

BRIDGE, J. S. & LEEDER, M .R. 1979. A simulation model of alluvial stratigraphy. *Sedimentology*, **26,** 617–644.

BULL, W .B. 1972. Recognition of alluvial fan deposits in the stratigraphic record. *In*: RIGBY, J.K. & HAMBLIN, W. K. (eds) *Recognition of Ancient Sedimentary Environments.* Society of Economic Paleontologists and Mineralogists Special Publications, **16,** 63–83.

BURBANK, D. W. & VERGÉS, J. 1994. Reconstruction of topography and related depositional systems during active thrusting. *Journal of Geophysical Research,* **99,** 20281–20297.

——, BECK, R. A., RAYNOLDS, R. G. H., HOBBS, R. & TAHIRKHELI, R. A. K. 1988. Thrusting and gravel progradation in foreland basins: a test of

post-thrusting gravel dispersal. *Geology,* **16,** 1143–1146.

——, MEIGS, A. & BROZOVIĆ, N. 1996. Interactions of growing folds and coeval depositional systems. *Basin Research,* **8,** 199–223.

——, PUIGDEFÀBREGAS, C. & MUÑOZ, J. A. 1992*b*. The chronology of the Eocene tectonic and stratigraphic development of the eastern Pyrenean foreland basin, northeast Spain. *Geological Society of America Bulletin,* **104,** 1101–1120.

——, VERGÉS, J., MUÑOZ, J. A. & BENTHAM, P. 1992*a*. Coeval hindward- and forward-imbricating thrusting in the south-central Pyrenees, Spain: timing and rates of shortening and deposition. *Geological Society of America Bulletin,* **104,** 3–17.

COLOMBO, F. 1994. Normal and reverse unroofing sequences in syntectonic conglomerates as evidence of progressive basinward deformation. *Geology,* **22,** 235–238.

—— & VERGÉS, J. 1992. Geometria del margen S.E. de la Cuenca del Ebro: discordancias progresivas en el Grupo Scala Dei, Serra de La Llena (Tarragona). *Acta Geológica Hispànica,* **27,** 33–53.

CONEY, P. J., MUÑOZ, J. A., MCCLAY, K. R. & EVENCHICK, C. A. 1996. Syntectonic burial and post-tectonic exhumation of the southern Pyrenees foreland fold-thrust belt. *Journal of the Geological Society, London,* **153,** 9–16.

CURRAY, J. R. 1956. The analysis of two-dimensional orientation data. *Journal of Geology,* **64,** 117–131.

DAHLSTROM, C. D. A. 1969. Balanced cross sections. *Canadian Journal of Earth Sciences,* **6,** 743–757.

DECELLES, P. G., GRAY, M. B., RIDGWAY, K. D., COLE, R. B., PIVNIK, D. A., PEQUERA, N. & SRIVASTAVA, P. 1991*a*. Controls on synorogenic alluvial-fan architecture, Beartooth Conglomerate (Palaeocene), Wyoming and Montana. *Sedimentology,* **38,** 567–590.

——, ——, ——, ——, SRIVASTAVA, P., PEQUERA, N. & PIVNIK, D. A. 1991*b*. Kinematic history of a foreland uplift from Paleocene synorogenic conglomerate, Beartooth Range, Wyoming and Montana. *Geological Society of America Bulletin,* **103,** 1458–1475.

——, LAWTON, T. F. & MITRA, G. 1995. Thrust timing, growth of structural culminations, and synorogenic sedimentation in the type Sevier orogenic belt, western United States. *Geology,* **23,** 699–702.

DENNY, C. S. 1967. Fans and pediments. *American Journal of Science,* **265,** 81–105.

DOGLIONI, C. & PROSSER, G. 1997. Fold uplift versus regional subsidence and sedimentation rate. *Marine and Petroleum Geology,* **14,** 179–190.

ENGLAND, P. & MOLNAR, P. 1990. Surface uplift, uplift of rocks and exhumation of rocks. *Geology,* **18,** 1173–1177.

FORD, M., WILLIAMS, E. A., ARTONI, A., VERGÉS, J. & HARDY, S. 1997. Progressive evolution of a fault-related fold pair from growth strata geometries, Sant Llorenç de Morunys, SE Pyrenees. *Journal of Structural Geology,* **19,** 413–441.

FRIEND, P. F. 1989. Space and time analysis of river systems, illustrated by Miocene systems of the northern Ebro Basin in Aragon, Spain. *Revista de la Sociedad Geologica España,* **2,** 55–64.

GLOPPEN, T. G. & STEEL, R. J. 1981. The deposits, internal structure and geometry in six alluvial fan-fan delta bodies (Devonian – Norway) – a study in the significance of bedding sequence in conglomerates. *In*: ETHRIDGE, F. G. & FLORES, R. M. (eds) *Recent and Ancient Nonmarine Depositional Environments: Models for Exploration*. Society of Economic Paleontologists and Mineralogists, Special Publications, **31,** 49–69.

GONZÁLEZ, A., ARENAS, C. & PARDO, G. 1997. Discussion on syntectonic burial and post-tectonic exhumation of the southern Pyrenees foreland fold-thrust belt. *Journal of the Geological Society, London,* **154,** 361–365.

GUPTA, S. 1997. Himalayan drainage patterns and the origin of fluvial megafans in the Ganges foreland basin. *Geology,* **25,** 11–14.

HAUGHTON, P. D. W. 1989. Structure of some Lower Old Red Sandstone conglomerates, Kincardineshire, Scotland: deposition from late orogenic antecedent streams? *Journal of the Geological Society, London,* **146,** 509–525.

HEIN, F. J. & WALKER, R. G. 1977. Bar evolution and development of stratification in the gravelly braided Kicking Horse River, British Columbia. *Canadian Journal of Earth Sciences,* **14,** 562–570.

HEWARD, A. P. 1978. Alluvial fan sequence and megasequence models: with examples from Westphalian D-Stephanian B coalfields, northern Spain. *In*: MIALL, A.D. (ed.) *Fluvial Sedimentology*. Canadian Society of Petroleum Geologists, Memoirs, **5,** 669–702.

HIRST, J. P. P. & NICHOLS, G. J. 1986. Thrust tectonic controls on Miocene alluvial distribution patterns, southern Pyrenees. *In*: ALLEN, P. A. & HOMEWOOD, P. (eds) *Foreland Basins*. International Association of Sedimentologists, Special Publications, **8,** 247–258.

HOSSACK, J. R. 1979. The use of balanced cross-sections in the calculation of orogenic contraction. *Journal of the Geological Society, London,* **136,** 705–711.

HOVIUS, N. 1996. Regular spacing of drainage outlets from linear mountain belts. *Basin Research,* **8,** 29–44.

KOLTERMANN, C. E. & GORELICK, S. M. 1992. Paleoclimatic signature in terrestrial flood deposits. *Science,* **256,** 1775–1782.

LOWE, D. R. 1976. Grain flow and grain flow deposits. *Journal of Sedimentary Petrology,* **46,** 188–199.

MCPHERSON, J. G., SHANMUGAM, G. & MOIOLA, R. J. 1987. Fan-deltas and braid deltas: Varieties of coarse-grained deltas. *Geological Society of America Bulletin,* **99,** 331–340.

MATÓ, E., SAULA, E., MARTÍNEZ, A., MUÑOZ, J.A., VERGÉS, J. & ESCUER, J. 1994. *Memoria explicativa y cartografía geológica de la Hoja 293 (Berga) del mapa geológico de España Plan Magna a escala 1:50,000*. ITGE.

MEIGS, A.J., VERGÉS, J. & BURBANK, D.W. 1996. Ten-million-year history of a thrust sheet. *Geological Society of America Bulletin,* **108,** 1608–1625.

MELLERE, D. 1993. Thrust-generated, back-fill stacking of alluvial fan sequences, south-central Pyrenees, Spain (La Pobla de Segur Conglomerates).

In: FROSTICK, L.E. & STEEL, R.J. (eds) *Tectonic Controls and Signatures in Sedimentary Successions.* International Association of Sedimentologists, Special Publications, **20,** 259–276.

MILLÁN, H., AURELL, M. & MELENDEZ, A. 1994. Synchronous detachment folds and coeval sedimentation in the Prepyrenean External Sierras (Spain): a case study for tectonic origin of sequences and systems tracts. *Sedimentology,* **41,** 1001–1024.

MUÑOZ, J. A. 1992. Evolution of a continental collision belt: ECORS-Pyrenees crustal balanced cross-section. *In*: MCCLAY, K.R. (ed.) *Thrust Tectonics.* Chapman & Hall, London, 235–246.

NEMEC, W. & POSTMA, G. 1993. Quaternary alluvial fans in southwestern Crete: sedimentation processes and geomorphic evolution. *In*: MARZO, M. & PUIGDEFÀBREGAS, C. (eds) *Alluvial Sedimentation.* International Association of Sedimentologists, Special Publications, **17,** 235–276.

—— & STEEL, R. J. 1984. Alluvial and coastal conglomerates: their significant features and some comments on gravelly mass-flow deposits. *In*: KOSTER, E. H. & STEEL, R. J. (eds) *Sedimentology of Gravels and Conglomerates.* Canadian Society of Petroleum Geologists, Memoirs, **10,** 1–31.

—— & —— (eds) 1988. *Fan Deltas: Sedimentology and Tectonic Settings.* Blackie and Son Ltd.

——, ——, POREBSKI, S. J. & SPINNANGR, Å. 1984. Domba Conglomerate, Devonian, Norway: process and lateral variability in a mass flow-dominated, lacustrine delta. *In*: KOSTER, E. H. & STEEL, R. J. (eds) *Sedimentology of Gravels and Conglomerates.* Canadian Society of Petroleum Geologists, Memoirs, **10,** 295–320.

NICHOLS, G. J. 1987*a*. Structural controls on fluvial distributary systems- the Luna System, northern Spain. *In*: ETHRIDGE, F .G., FLORES, R. M. & HARVEY, M. D. (eds) *Recent Developments in Fluvial Sedimentology.* Society of Economic Paleontologists and Mineralogists, Special Publications, **39,** 269–277.

—— 1987*b*. Syntectonic alluvial fan sedimentation, southern Pyrenees. *Geological Magazine,* **124,** 121–133.

PAOLA, C. 1988. Subsidence and gravel transport in alluvial basins. *In*: KLEINSPEHN, K. L. & PAOLA, C. (eds) *New Perspectives in Basin Analysis.* Springer-Verlag, New York, 231–244.

—— 1989. A simple basin-filling model for coarse-grained alluvial systems. *In*: CROSS, T.A. (ed.) *Quantitative Dynamic Stratigraphy.* Prentice Hall, Englewood Cliffs, N.J., 363–374.

——, HELLER, P. L. & ANGEVINE, C. L. 1992. The large-scale dynamics of grain-size variation in alluvial basins, 1: Theory. *Basin Research,* **4,** 73–90.

RIBA, O. 1967. Resultados de un estudio sobre el Terciario continental de la parte este de la depresión central catalana. *Acta Geológica Hispànica,* **2,** 1–6.

—— 1973. Las discordancias sintectónicas del Alto Cardener (Prepirineo catalán), ensayo de interpretación evolutiva. *Acta Geológica Hispànica,* **8,** 90–99.

—— 1976*a*. Tectonogenèse et Sedimentation: deux modèles de discordances syntectoniques pyrénéenes. *Bulletin du Bureau des Recherches Géologique et Minières 2ème sér Sect I,* **4,** 387–405.

—— 1976*b*. Syntectonic unconformities of the Alto Cardener, Spanish Pyrenees: a genetic interpretation. *Sedimentary Geology,* **15,** 213–233.

——, REGUANT, S. & VILLENA, J. 1983. Ensayo de síntesis estratigráfica y evolutiva de la cuenca terciaria del Ebro. *In*: COUMBA, J. A. (ed.) *Libro Jubilar J.M. Ríos. Geología de España,* **II.**, IGME, Madrid, 131–159.

ROCKWELL, T. K., KELLER, E. A. & JOHNSON, D. L. 1985. Tectonic geomorphology of alluvial fans and mountain fronts near Ventura, California. *In*: MORISAWA, M. & HACK, J. T. (eds) *Tectonic Geomorphology.* Allen & Unwin, Boston, 183–207.

RUST, B. R. & KOSTER, E. H. 1984. Coarse Alluvial Deposits. *In*: WALKER, R. G. (ed.) *Facies Models.* Geological Association of Canada, Toronto, 53–69.

SÁEZ, A. 1987. *Estratigrafía y sedimentología de las formaciones lacustres del tránsito Eoceno-Oligoceno del NE de la cuenca del Ebro.* PhD thesis, Universitat de Barcelona.

SCHUMM, S.A. 1981. Evolution and response of the fluvial system, sedimentologic implications. *In*: ETHRIDGE, F.G. & FLORES, R.M. (eds) *Recent and Ancient Nonmarine Depositional Environments: Models for Exploration.* Society of Economic Paleontologists and Mineralogists, Special Publications, **31,** 19–29.

STEEL, R. J. & THOMPSON, D. B. 1983. Structures and textures in Triassic braided stream conglomerates ('Bunter' Pebble Beds) in the Sherwood Sandstone Group, North Staffordshire, England. *Sedimentology,* **30,** 341–367.

SUPPE, J., SÀBAT, F., MUÑOZ, J.A., POBLET, J., ROCA, E. & VERGÉS, J. 1997. Bed-by bed fold growth by kink-band migration: Sant Llorenç de Morunys, eastern Pyrenees. *Journal of Structural Geology,* **19,** 443–461.

TODD, S. P. 1989. Stream-driven, high-density gravelly traction carpets: possible deposits in the Trabeg Conglomerate Formation, SW Ireland and some theoretical considerations of their origin. *Sedimentology,* **36,** 513–530.

VERGÉS, J. 1993. *Estudi geològic del vessant sud del Pirineu oriental i central. Evolució cinemàtica en 3D.* PhD thesis, Universitat de Barcelona.

—— & RIBA, O. 1991. Discordancias sintectónicas ligadas a cabalgamientos: modelo cinemático. *Comunicaciones Congreso del Grupo Español del Terciario,* 341–345.

——, BURBANK, D. W. & MEIGS, A. 1996. Unfolding: An inverse approach to fold kinematics. *Geology,* **24,** 175–178.

WHEELER, H. E. & MALLORY, V. S. 1956. Factors in lithostratigraphy. *American Association of Petroleum Geologists Bulletin,* **40,** 2711–2723.

WHIPPLE, K. X. & TRAYLER, C. R. 1996. Tectonic control of fan size: the importance of spatially variable subsidence rates. *Basin Research,* **8,** 351–366.

WOLMAN, M. G. & MILLER, J. P. 1960. Magnitude and frequency of forces in geomorphic processes. *Journal of Geology,* **68,** 54–74.

Cenozoic Foreland Basins of Western Europe

edited by
A. Mascle (IFP, Rueil-Malmaison, France)
C. Puigdefàbregas (CSIC, Barcelona, Spain)
H. P. Luterbacher (University of Tübingen, Germany)
and
M. Fernàndez (CSIC, Barcelona, Spain)

The volume provides a modern synthesis of foreland basin stratigraphy and structural geology. It covers the foothills and foreland basins of the northwestern Alps, the Pyrenees and the Betic thrust belt. The multidisciplinary approach includes both sedimentological and structural studies, plus numerical modelling as a tool to quantify and integrate the geological data.

This book results from the Integrated Basin Studies Project, which was funded by the European Commission. More than 200 researchers from 38 institutions in 15 countries have collaborated in the IBS project. Several papers from outside the project have also been included to provide the reader with a more comprehensive overview of Western Europe's Cenozoic foreland basins. This volume concentrates on scientific research, but many oil companies are actively exploring the foothills of thrust belts throughout the world, and this book will be an invaluable reference work for exploration geologists as well as for academics.

- 442 pages
- 18 chapters
- 233 illustrations including foldouts
- index

Cover picture: Western edge of the Vercors Massif, Western Alps, SE France: frontal thrust and fold in the Royan Valley leading to a 1000 m uplift of Urgonian (Barremian–Aptian) shallow water massive limestones in late Miocene–early Pliocene times. Photo: A. Mascle, IFP School.

ISBN 1-86239-015-0